

Revisiting Lossless Convexification: Theoretical Guarantees for Discrete-time Optimal Control Problems

Dayou Luo ^a, Kazuya Echigo ^b, and Behçet Açıkmeşe ^b

^a*Department of Applied Mathematics, University of Washington, Seattle, WA, 98195*

^b*William E. Boeing Department of Aeronautics and Astronautics, University of Washington, Seattle, WA, 98195*

Abstract

Lossless Convexification (LCvx) is a modeling approach that transforms a class of nonconvex optimal control problems, where nonconvexity primarily arises from control constraints, into convex problems through convex relaxations. These convex problems can be solved using polynomial-time numerical methods after discretization, which converts the original infinite-dimensional problem into a finite-dimensional one. However, existing LCvx theory is limited to continuous-time optimal control problems, as the equivalence between the relaxed convex problem and the original nonconvex problem holds only in continuous-time. This paper extends LCvx to discrete-time optimal control problems by classifying them into normal and long-horizon cases. For normal cases, after an arbitrarily small perturbation to the system dynamics (recursive equality constraints), applying the existing LCvx method to discrete-time problems results in optimal controls that meet the original nonconvex constraints at all but no more than $n_x - 1$ temporal grid points, where n_x is the state dimension. For long-horizon cases, the existing LCvx method fails, but we resolve this issue by integrating it with a bisection search, leveraging the continuity of the value function from the relaxed convex problem to achieve similar results as in normal cases. This paper improves the theoretical foundation of LCvx, expanding its applicability to real-world discrete-time optimal control problems.

1 Introduction

Lossless Convexification (LCvx) is a technique that reformulates a class of nonconvex continuous-time optimal control problems—where nonconvexity primarily stems from control constraints—into convex problems through novel relaxation methods. Pontryagin’s maximum principle provides a theoretical guarantee for this approach, ensuring that the solution to the relaxed convex problem still satisfies the constraints of the original nonconvex problem [Açıkmeşe and Ploen, 2005, Berkovitz, 1975]. By converting complex nonconvex problems into convex ones, this relaxation reduces computational cost as the resulting convex problem, after being discretized into a finite-dimensional form, can then be efficiently solved using standard solvers such as ECOS [Domahidi et al., 2013] or Mosek [ApS, 2019] in polynomial time to a specified accuracy [Nemirovski, 2004].

LCvx research has been active for the past decade, and it has proven useful in numerous applications [Malyuta et al., 2022]. The initial application of the LCvx method targeted Mars pinpoint landings [Açıkmeşe and Ploen, 2005, 2007], where the nonzero lower bound on the magnitude of the control input vector led to

nonconvex control constraints. Later, the LCvx family has been generalized to handle a wide range of continuous-time optimal control problems, including but not limited to those with generalized nonconvex input constraints [Açıkmeşe and Blackmore, 2011], input pointing constraints [Carson et al., 2011], integer constraints [Harris, 2021, Echigo et al., 2023, 2024], as well as problems with additional convex affine and quadratic state constraints [Harris and Açıkmeşe, 2013, 2014]. Moreover, the efficacy of the LCvx method has also been tested in real-world experiments [Açıkmeşe et al., 2012, 2013] and is now being used as a baseline for Moon landing applications [Fritz et al., 2022, Shaffer et al., 2024].

Despite the success of LCvx in real-world applications, its theoretical results have a gap, which may have practical implications for its use. While LCvx theory establishes an equivalence between a continuous-time nonconvex optimal control problem and its convex relaxation, both remain continuous-time problems and cannot be directly solved by numerical solvers, which handle only finite-dimensional problems. To address this, we discretize both problems into finite-dimensional, discrete-time versions [Açıkmeşe and Blackmore, 2011]. However, this discretization introduces additional challenges, as LCvx theory does not guarantee that the opti-

* Corresponding author Dayou Luo.

mal solution of the discretized convex problem satisfies the constraints of the discretized nonconvex problem.

In fact, the optimal solution of the discrete-time convex relaxed problem can violate the constraints of the original discrete-time nonconvex problem. In this paper, we provide examples where the optimal solution of the relaxed convex problem violates the nonconvex constraints of the original problem at single, multiple, or all temporal grid points. These examples emphasize the necessity of establishing a solid theory for directly applying the LCvx method to discrete-time nonconvex optimal control problems.

Instead of considering a general class of nonconvex control constraints, we focus on a simple problem where the lower bound of the nonzero norm on the control input magnitude is the sole source of nonconvexity. Here, the input magnitude is defined by a convex function of the input variable. We chose this problem because it can demonstrate the essence of LCvx method without introducing excessive mathematical complexity. The application of the LCvx method to a broader class of nonconvex problems will be explored in future studies.

The primary goal of this paper is to develop a new LCvx method that integrates the existing LCvx method with a bisection search. Additionally, we establish a comprehensive proof framework to validate this method for discrete-time nonconvex optimal control problems. In this framework, we classify these problems into two categories: normal cases and long-horizon cases. Long-horizon cases arise when the control horizon is sufficiently long to admit an optimal solution for the convexified problem, but the input magnitude of this solution consistently violates the nonconvex input constraints throughout the trajectory. All other problems are classified as normal cases. For normal cases, our method is identical to the existing LCvx method, as the existing approach has demonstrated effective performance for such cases [Açikmeşe and Ploen, 2005, 2007]. However, in long-horizon cases, the existing approach fails to provide feasible solutions for the nonconvex problem. To address this, we introduce a bisection search strategy specifically designed to handle long-horizon cases.

For the normal case, we provide a theoretical guarantee for applying the existing LCvx method to discrete-time optimal control problems by proving a bound on the number of points where the optimal solution to the convexified problem can violate the original nonconvex constraints. Specifically, we show that, after an arbitrarily small perturbation to the dynamics, the optimal solution to the convexified problem violates nonconvex constraints at no more than $n_x - 1$ temporal grid points, where n_x is the state dimension. Furthermore, we show that the perturbed problem maintains all necessary assumptions from the relaxed convex problem and we establish bounds on the impact of the perturbation. Numerical examples are also provided to demonstrate the necessity of the perturbation and the tightness of the upper bound. Our proof technique is closely related to

the discretized Pontryagin’s Maximum Principle [Sethi, 2021, Canon et al., 1970], as both approaches are based on the Lagrangian function for finite-dimensional optimal control problems. However, unlike the discretized Pontryagin’s Maximum Principle, our method does not involve the use of the Hamiltonian.

In contrast, the existing LCvx method does not work for long-horizon cases. To address this, we design a new LCvx method by combining the earlier LCvx method with a bisection search. This approach is motivated by the fact that existing LCvx theory requires strict transversality assumptions ([Malyuta et al., 2022, Condition 2], [Açikmeşe and Blackmore, 2011, Condition 2]), which fail in long-horizon cases. To overcome this, we divide the control horizon into two phases. In the first phase, we use an arbitrary feasible control input to ensure minimum cost. The final state of the first phase is then used as the initial state for the second phase, where we apply the existing LCvx method to the resulting nonconvex optimal control problem. We expect the control horizon for the second phase to be short enough to satisfy the transversality assumption and belong to normal cases, while still being long enough to maintain minimum input cost. To achieve this balance, we developed a bisection search to find the optimal transition time between phases, based on the fact that the value function of the resulting convex optimal control problem for the entire trajectory is continuous. By employing a bisection search, the second-phase control problem falls into the normal case category, enabling us to directly apply the theoretical results of normal cases to long-horizon problems. We note that another method in the LCvx family also uses the bisection search [Kunhippurayil et al., 2021] for continuous-time systems. The main distinction of our work is that we focus on discrete-time optimal control problems, including terminal costs in the objective function, and impose affine constraints on the terminal state.

Statement of Contributions: In this paper, we develop a new LCvx method for discrete-time nonconvex optimal control problems, bridging the gap between LCvx theory and its real-world applications. Specifically, our contributions are as follows.

First, we develop a new method and proof framework for discrete-time optimal control problems, which differs from previous LCvx research and other asymptotic theories for discretizations of continuous-time optimal control [Ober-Blobaum et al., 2011, Lee et al., 2022]. By focusing on discrete-time settings, we can provide a tight upper bound for the number of temporal grid points at which the optimal control violates the nonconvex constraints after applying the LCvx method.

Second, our proof framework employs linear algebra and finite-dimensional convex analysis, thus avoiding the need for infinite-dimensional mathematical tools such as Pontryagin’s maximum principle. This approach not only simplifies the theoretical development but also offers a fresh perspective on the mechanism of LCvx.

Third, our proof framework eliminates the requirement for the transversality assumption found in earlier LCvx theories ([Malyuta et al., 2022, Condition 2] and [Açikmeşe and Blackmore, 2011, Condition 2]), an assumption that is often difficult to verify before computation. This removal makes our method more applicable to real-world applications.

Road map: In Section 2, we review the background of LCvx research and define the optimization problem under consideration. Next, in Section 3, we provide an intuitive explanation of the mechanism of LCvx using convex analysis techniques and define the mathematical criteria for normal cases and long-horizon cases. In Section 4, we discuss the validity of LCvx for normal cases, define perturbations to the discrete dynamics, and provide theoretical guarantees for the LCvx method on the perturbed nonconvex optimal control problem. In Section 5, we address the long-horizon case and propose a bisection search algorithm for these cases. Finally, in Section 6, we present numerical experiments to demonstrate counterexamples where the LCvx method is invalid and showcase the perturbation and bisection search algorithms.

1.1 Notation

In the remainder of this discussion, we adopt the following notation. The set of integers $\{a, a+1, \dots, b-1, b\}$ is denoted by $[a, b]_{\mathbb{N}}$. The set of real numbers is denoted by \mathbb{R} , the set of real $n \times m$ matrices by $\mathbb{R}^{n \times m}$, and the set of real n -dimensional vectors by \mathbb{R}^n . Vector inequalities are defined elementwise. For matrices A_1, A_2, \dots, A_n , where each matrix A_i has the same number of rows, we denote the horizontal concatenation of these matrices by (A_1, A_2, \dots, A_n) . This operation results in a matrix formed by placing matrices A_1 through A_n side by side, from left to right. The Euclidean norm for vectors and matrices is denoted by $\|\cdot\|$, and the absolute value by $|\cdot|$. For a matrix A , $\exp(A)$ denotes the matrix exponential of A , with the definition available in [Chen, 1984] and $\text{rank}(A)$ denotes the rank of matrix A . For a convex set \mathbb{D} , the normal cone at the point z is denoted by $N_{\mathbb{D}}(z)$, with the definition found in [Borwein and Lewis, 2006, Chapter 2.1]. For a function $f(x, y)$ convex in (x, y) , $\partial_x f(x, y)$ and $\partial_y f(x, y)$ represent the subgradient of f with respect to the variables x and y separately, as defined in [Boyd and Vandenberghe, 2004]. For a differentiable function $f(x, y)$, $\nabla_x f(x, y)$ and $\nabla_y f(x, y)$ denote the partial derivative of f with respect to x and y separately. Finally, $\text{Prob}(E)$ denotes the probability that certain events E occur.

2 Background

In this section, we discuss the background of the LCvx method. Consider the optimization problem mentioned in [Malyuta et al., 2022, Problem 6], which includes no state constraints other than boundary conditions. We further simplify this problem to a time-invariant linear system without external disturbances. We believe that this basic form captures the essential

ideas of the LCvx method without adding mathematical complexity. This leads to the following optimal control problem:

Problem 1:

$$\begin{aligned} \min_{t_f, u, x} \quad & m(x(t_f)) + \int_0^{t_f} l_c(g_1(u(t))) dt, \\ \text{s. t.} \quad & \dot{x}(t) = A_c x(t) + B_c u(t), \\ & \rho_{\min} \leq g_1(u(t)), \quad g_0(u(t)) \leq \rho_{\max}, \text{ for } t \in [0, t_f] \\ & x(0) = x_{\text{init}}, \quad G(x(t_f)) = 0. \end{aligned}$$

Here, $m: \mathbb{R}^{n_x} \rightarrow \mathbb{R}$, $l_c: \mathbb{R} \rightarrow \mathbb{R}$, $g_0: \mathbb{R}^{n_u} \rightarrow \mathbb{R}$, and $g_1: \mathbb{R}^{n_u} \rightarrow \mathbb{R}$ are assumed to be convex C^1 smooth functions. $G: \mathbb{R}^{n_x} \rightarrow \mathbb{R}^{n_g}$ is an affine map. The state trajectory $x: [0, t_f] \rightarrow \mathbb{R}^{n_x}$ and the control input trajectory $u: [0, t_f] \rightarrow \mathbb{R}^{n_u}$ satisfy a continuous ordinary differential equation constraint. The condition $G(x(t_f)) = 0$ represents the boundary condition for the state trajectory x . $A_c \in \mathbb{R}^{n_x \times n_x}$ and $B_c \in \mathbb{R}^{n_x \times n_u}$ are constant matrices. $t_f \in \mathbb{R}$ is a free flight time and $x_{\text{init}} \in \mathbb{R}^{n_x}$ is a fixed initial state. $\rho_{\min} \in \mathbb{R}$ and $\rho_{\max} \in \mathbb{R}$ are fixed constants. The nonconvexity of Problem 1 arises solely from potentially nonconvex constraints $\rho_{\min} \leq g_1(u(t))$. The functions g_0 and g_1 characterize the magnitude of the input variable. A classic realization for both is to use the norm function, ensuring that the feasible region of Problem 1 meets the condition $\rho_{\min} \leq \|u(t)\| \leq \rho_{\max}$ for all t . These constraints arise from planetary soft landing applications, where the net thrust of rocket engines must exceed a positive lower bound to prevent shutdown [Açikmeşe and Ploen, 2005].

The LCvx technique introduced in [Açikmeşe and Blackmore, 2011] considers the following convex relaxation of the Problem 1:

Problem 2:

$$\begin{aligned} \min_{t_f, \sigma, u, x} \quad & m(x(t_f)) + \int_0^{t_f} l_c(\sigma(t)) dt, \\ \text{s. t.} \quad & \dot{x}(t) = A_c x(t) + B_c u(t), \\ & \rho_{\min} \leq \sigma(t), \quad g_0(u(t)) \leq \rho_{\max}, \quad g_1(u(t)) \leq \sigma(t), \\ & x(0) = x_{\text{init}}, \quad G(x(t_f)) = 0, \end{aligned}$$

where $\sigma: [0, t_f] \rightarrow \mathbb{R}$ is a slack variable introduced to convexify Problem 1. Because Problem 2 is a convex relaxation of Problem 1, the optimal value of the former serves as a lower bound for that of the latter. Theorem [Açikmeşe and Blackmore, 2011, Theorem 2] demonstrates that, under certain assumptions, an optimal solution to Problem 2 satisfies the constraints of Problem 1 almost everywhere, making it an optimal solution to Problem 1 as well.

Now, we consider the discretized, finite-dimensional, versions of Problem 1 and Problem 2. We apply a temporal discretization with zero-order hold for both infinite-dimensional problems to solve them numerically [Açikmeşe and Ploen, 2005, 2007, Açikmeşe and Blackmore, 2011]. Meanwhile, having a free final time t_f can undermine the convexity of the resulting optimization problem. To address this, a commonly used

method is to apply a line search for t_f . By solving the discretized relaxed problem for each t_f , one can find a t_f with the smallest objective value [Açikmeşe and Ploen, 2007]. Hence, in the rest of this paper, we only consider the cases where t_f is fixed.

With the following solution variables:

$$\begin{aligned} x &= \{x_1, x_2, \dots, x_{N+1}\}, \quad x_i \in \mathbb{R}^{n_x} \text{ for } i \in [1, N+1]_{\mathbb{N}} \\ u &= \{u_1, u_2, \dots, u_N\}, \quad u_i \in \mathbb{R}^{n_u} \text{ for } i \in [1, N]_{\mathbb{N}} \\ \sigma &= \{\sigma_1, \sigma_2, \dots, \sigma_N\}, \quad \sigma_i \in \mathbb{R} \text{ for } i \in [1, N]_{\mathbb{N}}. \end{aligned}$$

The discretized version of Problem 1 is:

Problem 3:

$$\begin{aligned} \min_{x, u} \quad & m(x_{N+1}) + \sum_{i=1}^N l_i(g_1(u_i)) \\ \text{s. t.} \quad & x_{i+1} = A_d x_i + B_d u_i, \quad i \in [1, N]_{\mathbb{N}} \\ & g_0(u_i) \leq \rho_{\max}, \quad g_1(u_i) \geq \rho_{\min}, \quad i \in [1, N]_{\mathbb{N}} \\ & x_1 = x_{\text{init}}, \quad G(x_{N+1}) = 0. \end{aligned}$$

The sum of $l_i: \mathbb{R} \rightarrow \mathbb{R}$ is an approximation for the integral term in the objective function of Problem 1. Matrices $A_d \in \mathbb{R}^{n_x \times n_x}$ and $B_d \in \mathbb{R}^{n_x \times n_u}$ for this discretized problem are given as [Chen, 1984]:

$$A_d = \exp\left(A_c \frac{t_f}{N}\right), \quad B_d = \int_0^{t_f/N} \exp(A_c \tau) d\tau B_c.$$

Since we mainly work with the discretized problem, we simplify the notation by using A for A_d and B for B_d . Condition $G(x_{N+1}) = 0$ is denoted as the boundary condition, $x_{i+1} = Ax_i + Bu_i$ as the dynamics constraints, and $m(x_{N+1}) + \sum_i l_i(\sigma_i)$ as the object function.

The discretized version of Problem 2 is:

Problem 4:

$$\begin{aligned} \min_{x, u, \sigma} \quad & m(x_{N+1}) + \sum l_i(\sigma_i) \\ \text{s. t.} \quad & x_{i+1} = Ax_i + Bu_i, \quad i \in [1, N]_{\mathbb{N}} \\ & \rho_{\min} \leq \sigma_i, \quad g_0(u_i) \leq \rho_{\max}, \quad g_1(u_i) \leq \sigma_i, \quad i \in [1, N]_{\mathbb{N}} \\ & x_1 = x_{\text{init}}, \quad G(x_{N+1}) = 0. \end{aligned}$$

Problem 4 can be understood as the result of applying the LCvx method to Problem 3. Since Problem 4 is a relaxation of Problem 3, its optimal value serves as a lower bound for that of Problem 3.

Motivated by previous LCvx research on continuous problems, a natural question arises: does the optimal solution to Problem 4 satisfy the constraints of Problem 3? However, this relationship does not hold in general. The numerical counterexamples in Section 6 show that the solution to Problem 4 often does not satisfy the constraints of Problem 3 at certain temporal grid points. Therefore, an optimal solution to Problem 4 is not guaranteed to solve Problem 3. As a result, we shifted our focus to a revised question. At how many temporal grid points can the solution to Problem 4 potentially violate the constraints of Problem 3, thereby invalidating LCvx? Here, we define the validity of LCvx at grid point i as:

Definition 1 *The LCvx method is valid at a grid point i if the control input u_i satisfies $g_0(u_i) \leq \rho_{\max}$ and*

$$g_1(u_i) \geq \rho_{\min}.$$

We will later prove that, with reasonable assumptions on Problem 4 and with arbitrarily small random perturbations to the discrete dynamics, LCvx is invalid at most at $n_x - 1$ temporal grid points, where n_x denotes the dimension of the variable x .

Before the theoretical discussion, we provide some definitions and assumptions for the problem 4 required for our discussion.

Assumption 2 *$l_i(\cdot)$ is C^1 smooth, and increases monotonically on $[\rho_{\min}, \infty)$. m is C^1 smooth. Set $\{u | g_1(u_i) \leq \rho_{\min} \text{ for all } i\}$ is nonempty. Set $\{u | g_0(u_i) \leq \rho_{\max} \text{ for all } i\}$ is a nonempty compact set. For a control at temporal grid point i , $g_0(u_i) = \rho_{\max}$ implies $g_1(u_i) \geq \rho_{\min}$.*

Note that if $\{u | g_1(u_i) \leq \rho_{\min} \text{ for all } i\}$ is empty, LCvx is trivially valid. The last part of Assumption 2 indicates that in Problem 3, $\{u | g_1(u_i) \leq \rho_{\min} \text{ for all } i\} \subset \{u | g_0(u_i) \leq \rho_{\max} \text{ for all } i\}$. A similar assumption is required in [Açikmeşe and Blackmore, 2011]. For further details, see the discussion under [Açikmeşe and Blackmore, 2011, Equation (4)].

We also require that the dynamical system in Problem 4 is controllable:

Assumption 3 (Controllability) *For matrices A and B in Problem 4,*

$$\text{rank} \begin{pmatrix} B & AB & \dots & A^{n_x-1}B \end{pmatrix} = n_x,$$

i.e., the matrix pair $\{A, B\}$ is controllable.

The controllability of the discretized system is closely related to that of the continuous dynamical system. Under mild assumptions, it has been shown that if the continuous dynamical system is controllable, then its discretized counterpart is also controllable [Chen, 1984, Theorem 6.9].

We now introduce some notation for further assumptions. Since the constraints on (u, σ) in Problem 4 are identical at each temporal grid point, we define $V :=$

$$\{(\bar{u}, \bar{\sigma}) \in \mathbb{R}^{n_u} \times \mathbb{R} \mid \rho_{\min} \leq \bar{\sigma}, \quad g_0(\bar{u}) \leq \rho_{\max}, \quad g_1(\bar{u}) \leq \bar{\sigma}\},$$

so that the constraint in Problem 4 can be expressed as $(u_i, \sigma_i) \in V$ for all i . The set V is convex as g_0 and g_1 are convex functions. Moreover, we define $V(\cdot)$ as

$$V(\bar{\sigma}) := \{\bar{u} \in \mathbb{R}^{n_u} \mid g_0(\bar{u}) \leq \rho_{\max}, \text{ and } g_1(\bar{u}) \leq \bar{\sigma}\},$$

i.e. $V(\bar{\sigma})$ is a slice of V at a specific value of $\bar{\sigma} \in \mathbb{R}$. The definition of $V(\cdot)$ establishes a sufficient condition for the validity of LCvx for certain u_i :

Lemma 4 *Under Assumption 2, if a control \bar{u} lies on the boundary of $V(\bar{\sigma})$ with $\bar{\sigma} \geq \rho_{\min}$, \bar{u} satisfies the constraints in Problem 3, i.e. $g_0(\bar{u}) \leq \rho_{\max}$ and $g_1(\bar{u}) \geq \rho_{\min}$.*

PROOF. The continuity of g_0 and g_1 implies that either $g_0(\bar{u}) = \rho_{\max}$ or $g_1(\bar{u}) = \bar{\sigma}$ holds: If neither condition is met, we can find an open neighborhood of \bar{u}

where $g_0(u) < \rho_{\max}$ and $g_1(u) < \bar{\sigma}$ for all u in this neighborhood. This contradicts the requirement of the theorem that \bar{u} is on the boundary of $V(\bar{\sigma})$. Therefore, when $\bar{\sigma} \geq \rho_{\min}$, under Assumption 2, the conditions $g_0(\bar{u}) = \bar{\sigma}$ or $g_1(\bar{u}) = \rho_{\max}$ ensure that $g_0(\bar{u}) \geq \rho_{\min}$. Consequently, \bar{u} satisfies both the convex and nonconvex constraints of Problem 3. \square

To define other assumptions, we need to further simplify the notation for Problem 4. Let $z := (x, u, \sigma) \in \mathbb{R}^{n_z}$ with $n_z = (N+1)n_x + Nn_u + N$. We denote the object function as $\Phi: \mathbb{R}^{n_z} \rightarrow \mathbb{R}$ and encapsulate the dynamics and boundary conditions into an affine constraint $H(z) = 0$, where $H: \mathbb{R}^{n_z} \rightarrow \mathbb{R}^{n_H}$ and n_H represents the total number of equality constraints. The remaining inequality constraints are written within the convex set $\tilde{V} = \{(x, u, \sigma) \in \mathbb{R}^{n_z} \mid (u_i, \sigma_i) \in V \text{ for all } i\}$. Thus, Problem 4 can be represented as:

Problem 5:

$$\begin{aligned} \min_z \quad & \Phi(z) \\ \text{s. t.} \quad & H(z) = 0, \quad z \in \tilde{V}. \end{aligned}$$

Since H is an affine function, the Jacobian of H , denoted as $\nabla H(z)$, is a constant matrix. Therefore, by eliminating the equations in H if necessary, $\nabla H(z)$ becomes a matrix of full rank. Since the dynamics equalities are designed to be full rank, any elimination of redundant constraints occurs only at the boundary condition and does not affect the dynamics equalities. After this elimination, we make the following assumption:

Assumption 5 For Problem 5, $\nabla H(z)$ has full row rank.

For the convex Problem 5, we further require the Slater condition:

Assumption 6 (Slater's condition) For Problem 5, there exists a vector z in the interior of \tilde{V} such that $H(z) = 0$

Assumption 6 is relatively modest. When both g_0 and g_1 are Euclidean norm functions, it is equivalent to having a control sequence $\|u_i\| < \rho_{\max}$ such that the trajectory generated by this u_i satisfies $G(x_{N+1}) = 0$. This holds when the optimal control problem is not overly constrained.

In the following discussion of this paper, Assumption 2, 3, 5, and 6 are valid for Problem 4 without further mentioning.

We conclude the background section with a continuity theorem, which is a major tool in our subsequent theoretical discussion. We begin by introducing a lemma which is a direct consequence of [Clarke et al., 2008, Lemma 3.3.3, Theorem 3.3.4]:

Lemma 7 Consider an optimization problem **Problem 6:**

$$\begin{aligned} \min_y \quad & M(y, p) \\ \text{s. t.} \quad & F(y, p) = 0, \quad y \in \Omega, \end{aligned}$$

where $y \in \mathbb{R}^{n_y}$, $p \in \mathbb{R}^{n_p}$. $M: \mathbb{R}^{n_y+n_p} \rightarrow \mathbb{R}$ and $F: \mathbb{R}^{n_y+n_p} \rightarrow \mathbb{R}^{n_F}$ are continuous with respect to (y, p) , and $\nabla_y F$ exists and is continuous with respect to (y, p) . Consider a solution (y^*, p_0) to the equality/constraint system

$$F(y^*, p_0) = 0, \quad y^* \in \Omega,$$

such that $\eta = 0$ is the unique solution to the following equation

$$0 \in \nabla_y F(y^*, p_0)^\top \eta + N_\Omega(y^*).$$

There exist $\delta, \xi > 0$ such that for any $p \in \mathbb{R}^{n_p}$ with $\|p - p_0\| < \xi$, there is a point $y \in \Omega$ satisfying $F(y, p) = 0$ and

$$\|y - y^*\| \leq \frac{\|F(y^*, p)\|}{\delta}.$$

We denote the optimum value to Problem 6 as $M^*(p)$. Our goal here is to show the continuity of M^* .

Theorem 8 Assume that the function F and an optimal solution (y^*, p_0) to Problem 6 satisfy all the assumptions in Lemma 7, Ω is compact, and M is a locally Lipschitz function with respect to (y, p) . Then, The optimal value function $M^*: \mathbb{R}^{n_p} \rightarrow \mathbb{R}$ to Problem 6 is continuous at p_0 .

PROOF. See Appendix 8.1. \square

3 Mechanism of LCvx

In this section, we provide a sufficient condition for the validity of LCvx and introduce the long-horizon cases and the normal cases for Problem 4.

To start, we define the Lagrangian of Problem 4 as follows:

$$\begin{aligned} L(x, u, \sigma; \eta, \mu_1, \mu_2) := & m(x_{N+1}) + \sum_{i=1}^N I_V(u_i, \sigma_i) \\ & + \sum_{i=1}^N l_i(\sigma_i) + \sum_{i=1}^N \eta_i^\top (-x_{i+1} + Ax_i + Bu_i + w_i) \\ & + \mu_1^\top (x_1 - x_{init}) + \mu_2^\top G(x_{N+1}), \end{aligned}$$

where I_V is the indicator function of set $V = \{(\bar{u}, \bar{\sigma}) \in \mathbb{R}^{n_u} \times \mathbb{R} \mid \rho_{\min} \leq \bar{\sigma}, g_0(\bar{u}) \leq \rho_{\max}, \text{ and } g_1(\bar{u}) \leq \bar{\sigma}\}$:

$$I_V(\bar{u}, \bar{\sigma}) = \begin{cases} 0 & \text{if } (\bar{u}, \bar{\sigma}) \in V, \\ +\infty & \text{otherwise,} \end{cases}$$

and the dual variable $\eta_i \in \mathbb{R}^{n_x}$ for $i = 1, 2, \dots, N$, $\eta = [\eta_1^\top, \eta_2^\top, \dots, \eta_N^\top]^\top \in \mathbb{R}^{n_x N}$, $\mu_i \in \mathbb{R}^{n_x}$, and $\mu_2 \in \mathbb{R}^{n_G}$.

Theorem 9 Suppose Assumption 6 holds, and let (x^*, u^*, σ^*) be a solution of Problem 4. Then, there exist dual variables $(\eta^*, \mu_1^*, \mu_2^*)$ such that

$$(x^*, u^*, \sigma^*) = \arg \min_{x, u, \sigma} L(x, u, \sigma; \eta^*, \mu_1^*, \mu_2^*). \quad (1)$$

PROOF. This follows directly from [Clarke, 2013, Theorem 9.4, 9.8 and 9.14]. \square

From equation (1), we derive:

$$\begin{aligned}\sigma^* &= \arg \min_{\sigma} L(x^*, u^*, \sigma; \eta^*, \mu_1^*, \mu_2^*), \\ u^* &= \arg \min_u L(x^*, u, \sigma^*; \eta^*, \mu_1^*, \mu_2^*), \\ x^* &= \arg \min_x L(x, u^*, \sigma^*; \eta^*, \mu_1^*, \mu_2^*).\end{aligned}\quad (2)$$

Since in the Lagrangian L , u_i only appears in terms $I_V(u_i, \sigma_i)$ and $\eta_i^\top B u_i$, we can write:

$$\begin{aligned}u_i^* &= \arg \min_{u_i} I_V(u_i, \sigma_i^*) + \eta_i^{*\top} B u_i \\ &= \arg \min_{u_i} I_V(\sigma_i^*)(u_i) + \eta_i^{*\top} B u_i.\end{aligned}\quad (3)$$

Equation (3) characterizes the relationship between u_i^* and σ_i^* . With (3) in hand, we discuss the sufficient condition for LCvx to be valid.

Theorem 10 (Sufficient Condition for LCvx)

Under Assumptions 2 and 6, the condition of $-B^\top \eta_i^$ being nonzero is sufficient for u_i to lie on the boundary of $V(\sigma_i^*)$, thus validating LCvx at the grid point i by Lemma 4. Furthermore, η_i^* is given by $\eta_i^* = A^{\top(N-i)} \eta_N^*$.*

PROOF. We first address the sufficient condition for u_i^* to lie on the boundary of $V(\sigma_i^*)$. Given that the right-hand side function of equation (3) is convex in u_i and u_i^* is a minimizer of this convex function, it follows that [Borwein and Lewis, 2006, Proposition 2.1.2]

$$-B^\top \eta_i^* \in N_{V(\sigma_i^*)}(u_i^*),$$

where $N_{V(\sigma_i^*)}(u_i)$ denotes the normal cone of the set $V(\sigma_i^*)$ at point u_i^* . The normal cone has nonzero elements only at the boundary points of $V(\sigma_i^*)$ [Bauschke, 2011, Corollary 6.44]. Hence, $-B^\top \eta_i^*$ being nonzero implies that u_i lies on the boundary of $V(\sigma_i^*)$. In such a case, LCvx is valid at node i according to Lemma 4.

For the evolution of η_i , considering equation (2), we take the partial derivative of L with respect to x_i for all i , yielding:

$$x_{N+1}: \quad \nabla m(x_{N+1}) + \mu_2^\top \nabla G(x_{N+1}) = \eta_N^*, \quad (4a)$$

$$x_i: \quad \eta_i^{*\top} A - \eta_{i-1}^{*\top} = 0, \quad (4b)$$

$$x_1: \quad \mu_1^\top + \eta_1^{*\top} A = 0.$$

Thus, iteratively applying (4b) leads to $\eta_i^* = A^{\top(N-i)} \eta_N^*$. The notation η_N in (4a), instead of η_{N+1} , is chosen to simplify the notation in subsequent derivations. \square

Remark 11 *Theorem 10 offers insight into why discrete LCvx is typically valid in applications. We start by designing a slack variable σ such that for a fixed σ , LCvx is valid as long as the control u is on the boundary of the feasible region defined by σ . Then, if a dual variable η_i^* is not in the left null space of matrix B , the corresponding control u lies on the boundary of the feasible region, thus validating LCvx.*

However, Theorem 10 does not guarantee the validity of LCvx, as $-B^\top \eta_i^* = 0$ can occur for some i . An obvious scenario for $\eta_i^* = 0$ is where $\eta_N^* = 0$. The following lemma characterizes this scenario.

Lemma 12 *Under Assumptions 2 and 6, if $\eta_N^* = 0$, then all $\sigma_i^* = \rho_{\min}$, and x_{N+1} must be an optimal solution to the following optimization problem:*

Problem 7:

$$\begin{aligned}\min_z \quad & m(x_{N+1}) \\ \text{s. t.} \quad & G(x_{N+1}) = 0.\end{aligned}$$

PROOF. From Theorem 10, $\eta_N^* = 0$ implies $\eta_i^* = 0$ for all i . By Theorem 9, we have

$$(\sigma^*, u^*) = \arg \min_{\sigma, u} \sum_{i=1}^N l_i(\sigma_i) + \sum_{i=1}^N I_V(u_i, \sigma_i).$$

Given Assumption 2, we have that $\sigma_i^* = \rho_{\min}$ and $u_i \in V(\rho_{\min})$.

We now prove the result on x_{N+1} . Equation (4a) ensures that

$$\nabla m(x_{N+1}) + \mu_2^\top \nabla G(x_{N+1}) = \eta_N^* = 0,$$

indicating that x_{N+1} is a KKT point of the convex optimization Problem 7 and thus a minimizer [Borwein and Lewis, 2006]. \square

Theorem 10 provides a sufficient condition for $\eta_N^* \neq 0$, leading to a natural division of Problem 4 into two scenarios:

Definition 13 *Problem 4 is defined as the long-horizon case if $\sigma_i^* = \rho_{\min}$ and x_{N+1} solves Problem 7. If these conditions are not satisfied, Problem 4 is classified as the normal case.*

The term long-horizon is used because $\eta_N^* = 0$ typically occurs when the control horizon is large. For a problem in the normal case, $\eta_N^* \neq 0$ according to Lemma 12. In previous LCvx research, $\eta_N^* \neq 0$ is usually ensured by assumptions, for example [Malyuta et al., 2022, Condition 2] and [Açikmeşe and Blackmore, 2011, Condition 2]. By identifying the long-horizon case, we can omit such types of assumptions.

In the next section, we discuss the theoretical guarantee for normal cases. The long-horizon cases will be left for the subsequent section.

4 LCvx on Normal cases

In this section, we concentrate on problems in the normal case and thus we assume that

Assumption 14 *Problem 4 is normal, i.e., either $\sigma_i > \rho_{\min}$ for some i or x_{N+1} is not the minimizer for Problem 7.*

As discussed previously, Assumption 14 implies that $\eta_N^* \neq 0$. A direct consequence of this assumption is:

Corollary 15 *Given Assumptions 2, 6 and 14, if the matrix A and B are invertible, then LCvx is valid at all temporal grid points.*

PROOF. When $\eta_N^* \neq 0$, since $\eta_i^* = A^{\top(N-i)} \eta_N^*$, a full rank matrix A ensures that η_i^* is non-zero for all i . The invertibility of B implies that $\eta_i^{*\top} B$ is non-zero for every

i , satisfying the conditions of Theorem 10 for LCvx to hold. \square

However, Corollary 15 might not always be applicable because it requires matrix B to be a square matrix, which means that the control and state dimensions must be equal; In practice, the state dimension often significantly exceeds the control dimension.

When the state dimension is larger than the control dimension, the validity of LCvx at all grid points is not guaranteed. Numerical examples in Section 6 show the invalidity of LCvx at multiple grid points for a non-square matrix B , even when the LCvx problem is normal. Therefore, we aim to establish a weaker statement: the original nonconvex constraints are violated at most at $n_x - 1$ temporal grid points, where n_x is the state dimension. However, this statement is still invalid as counterexamples exist (see Section 6.2). Thus, we consider an even weaker statement: after adding a random perturbation to the dynamics matrix A in Problem 4, the nonconvex constraints are violated at no more than $n_x - 1$ temporal grid points.

4.1 Perturbation

We define an arbitrarily small perturbation in the context of matrix A 's Jordan form, where A is defined in the dynamics constraints of Problem 3 and Problem 4:

Definition 16 Let matrix A 's Jordan form be

$$A = Q^{-1}JQ.$$

Assuming A has d distinct eigenvalues, we let these eigenvalues as $(\lambda_1, \dots, \lambda_d)$. Define $\tilde{A}(q)$ as a perturbation of A with respect to a vector $q = (q_1, q_2, \dots, q_d) \in \mathbb{R}^d$ if:

- $\tilde{A}(q) = Q^{-1}\tilde{J}Q$, where \tilde{J} is a Jordan matrix that is identical to J except for its diagonal elements.
- $\tilde{A}(q)$ has d eigenvalues $(\tilde{\lambda}_1, \dots, \tilde{\lambda}_d)$ such that $(\tilde{\lambda}_1, \dots, \tilde{\lambda}_d) = (\lambda_1, \lambda_2, \dots, \lambda_d) + (q_1, q_2, \dots, q_d)$.
- The index of Jordan blocks in \tilde{J} corresponding to $\tilde{\lambda}_i$ remains the same as in J corresponding to λ_i .

In essence, perturbing a matrix involves altering its eigenvalues. We intentionally preserve the Jordan form as it may convey important structural information about the dynamical system.

We now perturb Problem 4 by replacing the matrix A in the dynamic constraints with $\tilde{A}(q)$, where $\tilde{A}(q)$ represents a perturbation of A with respect to the vector $q \in \mathbb{R}^d$. Consequently, the optimization problem can be reformulated as follows:

Problem 8:

$$\begin{aligned} & \min_{x, u, \sigma} m(x_{N+1}) + \sum_{i=1}^N l_i(\sigma_i) \\ \text{s. t. } & x_{i+1} = \tilde{A}(q)x_i + Bu_i, \quad i \in [1, N]_{\mathbb{N}} \\ & \rho_{\min} \leq \sigma_i, \quad g_0(u_i) \leq \rho_{\max}, \quad g_1(u_i) \leq \sigma_i, \quad i \in [1, N]_{\mathbb{N}} \\ & x_1 = x_{init}, \quad G(x_{N+1}) = 0. \end{aligned}$$

If $q = 0$, we restore Problem 4.

In the remainder of this paper, $\mathbb{D} \subset \mathbb{R}^n$ denotes an n -dimensional unit cube, defined as $\mathbb{D} = \{x \in \mathbb{R}^n \mid -1 \leq x_i \leq 1, \forall i = 1, \dots, n\}$, where x_i is the i -th component of x in \mathbb{R}^n . For $\epsilon > 0$, we define the scaled cube $\epsilon\mathbb{D}$ as $\{x \in \mathbb{R}^n \mid -\epsilon \leq x_i \leq \epsilon, \forall i = 1, \dots, n\}$. The following theorem ensures that Assumptions 5, 3, 6, and 14 remain valid for the perturbed problem 8 under sufficiently small perturbations $q \in \epsilon\mathbb{D}$.

Lemma 17 Suppose that Assumptions 2, 3, 5, 6 and 14 hold for Problem 8 when $q = 0$. Then there exists an $\epsilon > 0$ such that for any $q \in \epsilon\mathbb{D} \subset \mathbb{R}^d$, Assumptions 2, 3, 5, 6 and 14 still hold for Problem 8 after perturbation by q .

PROOF. See Appendix 8.2. \square

Remark 18 In Lemma 17, we choose q from a cube region instead of the more conventional ball region, because we later want to generate q via a uniform distribution, and the cube region ensures independence for each dimension of q .

Lemma 17 establishes that Problem 8 follows the same assumptions as Problem 4. Therefore, all discussions in Section 3 regarding Problem 4 are also applicable to Problem 8 for sufficiently small q .

4.2 Quantify the LCvx invalidation

The goal for this section is to demonstrate that when the perturbation q is chosen randomly, the probability that LCvx is invalid for problem 8 at no more than $n_x - 1$ points is zero. To begin, we examine the necessary conditions for Problem 8 to violate the original nonconvex constraints at the grid points indexed by $P_1, P_2, \dots, P_k \in \mathbb{N}$.

Lemma 19 For Problem 8 with a fixed perturbation q , we define

$$S = \left(\tilde{A}(q)^{N-P_1} B \quad \tilde{A}(q)^{N-P_2} B \quad \dots \quad \tilde{A}(q)^{N-P_k} B \right),$$

where $P_1, P_2, \dots, P_k \in \mathbb{N}$ are temporal grid points. Suppose that Assumptions 2, 6, and 14 hold for Problem 8. If LCvx is invalid at the temporal grid points $P_1, P_2, \dots, P_k \in \mathbb{N}$, then the rank of S satisfies $\text{rank}(S) < n_x$.

PROOF. According to Theorem 10, the necessary condition for LCvx to be violated at the i -th point is: $\eta_i^\top B = 0$. Given that $\eta_i^\top = \eta_N^\top \tilde{A}(q)^{N-i}$, it follows that η_N^\top must lie in the left null space of $\tilde{A}(q)^{N-i} B$. Consequently, if LCvx is invalid at $\{P_1, P_2, \dots, P_k\}$, η_N^\top must lie in the left null space of the matrix S . According to Assumption 14, η_N is nonzero. Hence S has nontrivial left null space. Then $\text{rank}(S) < n_x$. \square

Now we have the main theorem.

Theorem 20 Given that Assumptions 2, 5, 6 and 14 hold for Problem 4, along with the controllability of $\{A, B\}$. Then, there exists an $\epsilon > 0$ such that if a vector $q \in \mathbb{R}^d$ is uniformly distributed over cube $\epsilon\mathbb{D} \in \mathbb{R}^d$, the

probability of the optimal trajectory for Problem 8 violating the nonconvex constraints in Problem 3 at more than $n_x - 1$ grid points is zero.

PROOF. See Appendix 8.3. The key to this proof is to use Lemma 19. We show that for a sufficiently small perturbation q and for arbitrary integers $1 \leq P_1 < P_2 < \dots < P_{n_x} < N + 1$, where N is the total amount of temporal grid points, the matrix S defined in Lemma 19 is of full rank with probability one. \square

Remark 21 *The perturbation mentioned in Theorem 20 is solely for the purposes of mathematical discussion and is not required in practical applications. However, such a perturbation is mathematically necessary. The numerical example in Section 6.2, artificially constructed as a counterexample, demonstrates that LCvx can become invalid at more than $n_x - 1$ nodes if no perturbation is applied. Furthermore, this numerical example also indicates that $n_x - 1$ is a tight upper bound for the number of temporal grid points at which LCvx becomes invalid, given that the control dimension is one.*

We also want to estimate the influence of the perturbation. Taking the control sequence that is optimum to Problem 8, and applying it to the unperturbed dynamics, we are expecting that when perturbation q is sufficiently small, the perturbation does not lead to a significant difference in the output of the unperturbed dynamics.

Theorem 22 *Suppose Assumptions 2, 5, 6 and 14 hold for Problem 8. Let the control sequence obtained by solving Problem 8 as $u(q)$ and apply this control to the unperturbed dynamics, leading to a trajectory*

$$\begin{aligned} \tilde{x}_{N+1}(q) &= x_1 + \sum_{i=1}^N A^{i-1} B u_i(q) \\ &= x_1 + \sum_{i=1}^N \tilde{A}^{i-1}(0) B u_i(q), \end{aligned}$$

where $u_i(q)$ is the control sequence $u(q)$ at the i -th temporal grid point. Then, for any $\delta > 0$, there exists an $\epsilon > 0$ such that for any $\|q\| < \epsilon$, $\tilde{x}_{N+1}(q)$ and $u(q)$ satisfy:

- $\|G(\tilde{x}_{N+1}(q))\| \leq \delta$,
- $m(\tilde{x}_{N+1}(q)) + \sum_{i=1}^N l_i(g_1(u_i(q))) \leq m_o^* + \delta$,

where m_o^* is the optimum value of the discretized nonconvex Problem 3.

PROOF. See Appendix 8.4. \square

5 LCvx on Long-horizon Cases

In this section, we address long-horizon cases. In such scenarios, the optimal control inputs of Problem 4 can violate the nonconvex constraints of Problem 3 at all temporal grid points, i.e., $g_1(u_i) < \rho_{\min}$ for all i . In this case, we expect that an optimal solution to the *continuous-time* nonconvex Problem 1 would have control inputs

$u(t)$ satisfying $g_1(u) = \rho_{\min}$, and the final state $x(t_f)$ is the optimal solution for Problem 7.

To find an optimal solution for the *continuous-time* nonconvex Problem 1, we adopt a strategy that involves dividing the trajectory into two phases, with the switching point between these phases denoted t_s . The first phase is defined on the interval $[0, t_s]$. In this phase, we set the control input $u : [0, t_s] \rightarrow \mathbb{R}^{n_u}$ to be constant, ensuring that $g_1(u) = \rho_{\min}$, while the state trajectory follows the continuous dynamics described in Problem 1. The final state of the first phase then serves as the initial state for the second phase. In the second phase, we formulate a discrete-time convex optimization problem by discretizing the continuous dynamics over $[t_s, t_f]$. The boundary state constraint is maintained, and the convexified control constraints are evaluated at temporal grid points.

Identifying the precise transition time, t_s , poses a challenge. We aim for t_s to be sufficiently long so that the discrete convex optimization problem in the second phase belongs to the normal cases. Simultaneously, t_s must be short enough to minimize the control and final state costs of the second phase. Hence, we adopt the bisection search method to determine t_s . We will demonstrate that the optimal total cost of the first and second phases is a continuous function of t_s , which justifies the use of the bisection search method. An optimal t_s should minimize the total cost while ensuring that the discrete convex LCvx problem in the second phase is normal. In particular, the continuous analog of this bisection search method approach is discussed in [Kunhippurayil et al., 2021].

As explored in Section 4, solving the discrete LCvx problem does not ensure LCvx validation at all temporal grid points. Thus, we aim to find a control sequence such that the constraint $\rho_{\min} + \epsilon \geq g_1(u_i) \geq \rho_{\min}$ for any arbitrarily small fixed $\epsilon > 0$ is violated at no more than $n_x - 1$ grid points after the perturbation described in Theorem 20. Additionally, x_{N+1} should be an optimal solution to Problem 7 up to any arbitrarily small fixed constant ϵ . The mathematical definition for this statement is available in Theorem 27.

Now, we mathematically define the bisection search method. In the first phase, we fix the control input as a constant $u_s \in \mathbb{R}^{n_u}$ over a duration $t_s \in \mathbb{R}$, with the initial condition $x_s \in \mathbb{R}^{n_x}$ provided in the original problem. The control u_s is chosen to ensure $g_1(u_s) = \rho_{\min}$. The continuous dynamics matrices are denoted as A_c and B_c . By plugging in u_s into the continuous dynamics, we determine the final state of the first phase, which also serves as the initial condition for the second phase:

$$x_{\text{init}}(t_s) = \exp(A_c t_s) x_s + \int_0^{t_s} \exp(A_c \tau) d\tau B_c u_s.$$

For the second phase, we define a discrete convexified optimization Problem 4, keeping the dynamics discretized as N pieces with zero-order hold control. The

discrete dynamics matrices are expressed as:

$$A(t_s) = \exp\left(A_c \frac{t_f - t_s}{N}\right),$$

$$B(t_s) = \int_0^{(t_f - t_s)/N} \exp(A_c \tau) d\tau B_c,$$

where $t_f - t_s$ is the amount of time remaining for the second phase.

Furthermore, we modify the objective function of Problem 4 by replacing $l_i(\sigma_i)$ with $l(\sigma_i) \times (t_f - t_s)/N$, where l is chosen such that its derivative on the domain of σ is lower-bounded by some $L_l > 0$. This adjustment simplifies the mathematical derivation. Theorem 27 justifies this modification, ensuring that the quality of the resulting trajectory and control variables remains unaffected.

The optimization problem for the second phase is then formulated as:

Problem 9:

$$\min_{x, u, \sigma} \quad m(x_{N+1}) + \sum_{i=1}^N l(\sigma_i) \frac{t_f - t_s}{N} + t_s l(\rho_{\min})$$

s. t. $x_{i+1} = A(t_s)x_i + B(t_s)u_i$, for $i \in [1, N]_{\mathbb{N}}$.

$\rho_{\min} \leq \sigma_i$, $g_0(u_i) \leq \rho_{\max}$, $g_1(u_i) \leq \sigma_i$,
for $i \in [1, N]_{\mathbb{N}}$.

$x_1 = x_{\text{init}}(t_s)$, $G(x_{N+1}) = 0$.

Here, we introduce a constant term $t_s l(\rho_{\min})$ to the objective function of the aforementioned optimization problem to account for the cost of the first phase. This addition simplifies the proof while leaving the optimal solution of the second phase unaffected. The value of the optimal objective function, denoted by $v(t_s)$, depends on t_s and represents the total cost of the flight, where the minimum value of $v(t_s)$ is $m^* + t_f l(\rho_{\min})$, with m^* being the optimal value of Problem 7. Our primary objective is to determine a t_s such that $v(t_s) < m^* + t_f l(\rho_{\min}) + \epsilon$, for a given and arbitrarily small $\epsilon > 0$. Additionally, to ensure the applicability of the theorems from the previous section, we require that Problem 9 satisfies the normal case condition.

To simplify the notation for Problem 9, we define $z = (x, u, \sigma)$, the object function as $M(z, t_s)$, and all affine equalities as $F(z, t_s) = 0$. The remaining inequality constraints are identical to the set \tilde{V} in (2). Thus, our problem can be represented as:

Problem 10:

$$\min_z \quad M(z, t_s)$$

s. t. $F(z, t_s) = 0$, $z \in \tilde{V}$.

The optimal value is a function of t_s , denoted as $v(t_s)$.

We require the following assumption for Problem 10.

Assumption 23 *Problem 4 belongs to the long-horizon case. Meanwhile, there exists a t_b such that $v(t_b) > m^* + t_f l(\rho_{\min})$. Assumptions 2, 3, 5, and 6 are valid for Problem 9 generated by $t_s \in [0, t_b]$.*

Lemma 24 *Assumption 23 ensures that Problem 9 generated by t_b has a non-zero η_N^* .*

PROOF. The condition $v(t_b) > m^* + t_f l(\rho_{\min})$ ensures that either x_{N+1} is not the solution to Problem 7, or at least one σ_i^* exceeds ρ_{\min} . In both cases, $\eta_N^* \neq 0$ follows by the contrapositive of Lemma 12. \square

Consequently, we have the following continuity result:

Lemma 25 *Assumption 23 ensures that $v(t)$ is continuous over $(0, t_b]$.*

PROOF. Assumption 23 guarantees that, for each t , solutions exist for Problem 10. For each t , we select one solution and denote it as $z^*(t)$. Consequently, we can apply Theorem 8 to Problem 10 at the point $(z^*(t), t)$ for all t , with the prerequisites of Theorem 8 being met by Assumption 23 and Lemma 29 in the Appendix. The compactness in Theorem 8 is satisfied by the same method used in Lemma 31. \square

Since $v(t)$ is a continuous function of t , we can apply the bisection search method to find the transition point. Under Assumption 23, $v(0) = m^* + t_f l(\rho_{\min})$, and $v(t_b) > m^* + t_f l(\rho_{\min})$, where m^* is the optimal value of Problem 7. We let $t_{\text{low}} = 0$ and $t_{\text{high}} = t_b$. In each iteration, we choose $t_{\text{mid}} = (t_{\text{low}} + t_{\text{high}})/2$. If $v(t_{\text{mid}}) > m^* + t_f l(\rho_{\min})$, we replace t_{high} with t_{mid} . Otherwise, we replace t_{low} with t_{mid} . The following theorem is a direct consequence of a standard bisection search method argument, the fact that $v(t)$ is continuous and Lemma 24.

Theorem 26 *Under Assumption 23, for any $\epsilon > 0$, the bisection search method finds a $t_s^* \in (0, t_b)$ ensuring the following inequality within finite iterations:*

$$m^* + t_f l(\rho_{\min}) < v(t_s^*) < m^* + t_f l(\rho_{\min}) + \frac{\epsilon}{2},$$

where m^* is the optimal value of Problem 7. Meanwhile, the Problem 10 generated by t_s^* is normal.

Since the Problem 10 generated by t_s^* is normal, we can now add the perturbation and apply the results from Theorem 20 and 22. As tuning the switch point changes the horizon and discretization of Problem 10, we cannot directly compare the solution of Problem 10 to that of the discrete Problem 3. Therefore, we directly compare the result of Problem 10 to that of the continuous-time Problem 1. Note that the best possible solution for Problem 1 is the one with control $g_1(u(t)) = \rho_{\min}$ for all t and $m(x(t_f))$ equal to m^* , where m^* is the optimal value of Problem 7. The next theorem shows that the solution of Problem 10 with perturbation achieves $m(x(t_f))$ almost equal to m^* , and $g_1(u_i)$ less than ρ_{\min} up to an arbitrarily small $\epsilon > 0$.

To do this, we need a few notations consistent with those of Theorem 20. Consider the Problem 9 generated

from t_s^* . We add a perturbation $q \in \mathbb{R}^d$ to the dynamics matrix $A(t_s^*)$ and denote the perturbed matrix as $\tilde{A}(t_s^*, q)$. The optimal solution of the resulting perturbed optimization problem is denoted as $(x(q), u(q), \sigma(q))$. If we plug in $u(q)$ into the original dynamics, we have

$$\begin{aligned}\tilde{x}_{N+1}(q) &= x_1 + \sum_{i=1}^N A(t_s^*)^{i-1} B(t_s^*) u_i(q) \\ &= x_1 + \sum_{i=1}^N \tilde{A}^{i-1}(t_s^*, 0) B(t_s^*) u_i(q)\end{aligned}$$

Here, $\tilde{x}_{N+1}(q)$ is denoted to be the endpoint of the propagated trajectory if we apply the control acquired from the perturbed problem to the original dynamics.

Theorem 27 *Assume Assumption 23 is valid, Choose a function $l: \mathbb{R} \rightarrow \mathbb{R}$ for Problem 9 such that the derivative of l is larger than some $L_l > 0$ within the domain of σ . Then, for any $\epsilon > 0$, we can acquire $t_s^* \in \mathbb{R}$ and $\delta > 0$ such that for any perturbation $q \in \mathbb{R}^d$ with $\|q\| < \delta$ applied to Problem 10 generated by t_s^* , the control $u(q)$ and the propagated trajectory $\tilde{x}_{N+1}(q)$ satisfies:*

- $\|G(\tilde{x}_{N+1}(q))\| \leq \delta$,
- $g_1(u_i) \geq \rho_{min}$ for all i up to $n_x - 1$ points with probability one.
- $\rho_{min} + \epsilon > g_1(u_i)$ for all i ,
- $m^* + \epsilon > m(\tilde{x}_{N+1}(q))$,

where m^* is the solution to Problem 7.

PROOF. See Appendix 8.5 \square

Theorem 27 guarantees the validity of adding perturbation to the dynamics. Consequently, we introduce Algorithm 1, which is capable of handling both normal and long-horizon cases. This algorithm provides a control sequence that at most violates the original nonconvex constraints at $n_x - 1$ grid points. In practical applications, the perturbation step is likely to remain deactivated since it serves primarily for theoretical completeness and is activated only in artificial edge cases.

6 Numerical Examples

In this section, we consider three illustrative numerical examples.

The first example involves a well-conditioned dynamics model that satisfies all assumptions outlined in Sections 3 and 4. The numerical experiment demonstrates that LCvx is invalid at one temporal grid point, indicating that the solution to Problem 4 may not necessarily be the solution of Problem 3.

The second example explores an artificial case, which, while not practical, is useful for illustration. In this case, LCvx is initially invalid at n_x points. Introducing a perturbation reduces this violation to $n_x - 1$ points, highlighting the necessity of a perturbation and the tightness of the $n_x - 1$ bound in Theorem 20.

The third example addresses a long-horizon case. It serves to demonstrate a typical long-horizon scenario

Algorithm 1 LCvx Method with Bisection for the Long Horizon Cases

Require: $A_c, B_c, A, B, u_s, x_s, \rho_{min}, \epsilon_t > 0, \epsilon_q > 0$

Ensure: Optimized time t_s , state x , control u , and slack variables σ

- 1: Set $t_{low} = 0, t_{high} = t_f, t_s^* = 0, x_{init} = x_s$
 - 2: Solve Problem 4 to obtain x, u, σ
 - 3: **if** $\sigma_i > \rho_{min}$ for some i or x_{N+1} doesn't solve Problem 7 **then**
 - 4: **if** the number of nodes that LCvx being invalid $\leq n_x - 1$ **then**
 - 5: **return** t_s^*, x, u, σ
 - 6: **else**
 - 7: Perturb the optimization Problem 4 with randomly generated $\|q\| \leq \epsilon_q$
 - 8: Solve the perturbed Problem 4 to obtain x, u, σ
 - 9: **return** t_s^*, x, u, σ
 - 10: **end if**
 - 11: **end if**
 - 12: Modify the object function l_i to $l(\sigma_i) \times (t_f - t_s)/N$ that satisfies assumption in Theorem 27
 - 13: Set $t_s = (t_{low} + t_{high})/2$
 - 14: **while** $(t_{high} - t_{low}) > \epsilon_t$ **do**
 - 15: Solve Problem 9 defined by t_s and u_s to obtain x, u, σ
 - 16: **if** $\sigma_i > \rho_{min}$ for some i or x_{N+1} doesn't solve Problem 7 **then**
 - 17: Set $t_{low}, t_{high} = t_{low}, t_s$
 - 18: **else**
 - 19: Set $t_{low}, t_{high} = t_s, t_{high}$
 - 20: **end if**
 - 21: $t_s = (t_{low} + t_{high})/2$
 - 22: **end while**
 - 23: $t_s^* = t_{high}$
 - 24: Solve Problem 9 defined by t_s^* to obtain x, u, σ .
 - 25: **if** the number of nodes that LCvx being invalid $\leq n_x - 1$ **then**
 - 26: **return** t_s^*, x, u, σ
 - 27: **else**
 - 28: Perturb the optimization Problem 9 by $\|q\| \leq \epsilon_q$ to obtain x, u, σ
 - 29: **return** t_s^*, x, u, σ
 - 30: **end if**
-

and the application of the bisection search method algorithm.

One can show that Assumptions 2, 3, 5, 6 and 14 are satisfied for the first and second example. Testing Slater's Condition in Assumption 23 directly for the third example is challenging as it requires verification for all $t_s \in [0, t_b]$. Developing a method to test such an assumption will be left for future research. Other conditions in Assumption 23 are satisfied for the third example.

For our numerical examples, we used Matlab and selected Mosek [ApS, 2019] as our convex solver, due to its high accuracy in solving convex optimization problems.

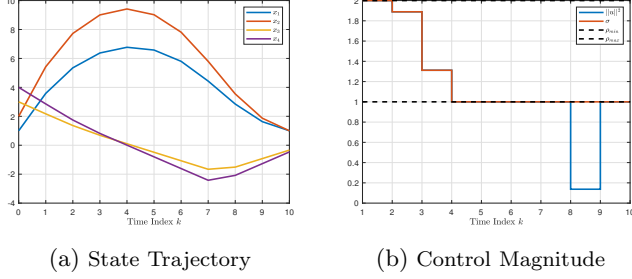


Fig. 1. State trajectory and control magnitude for a well-conditioned four-dimensional system over ten temporal grid points. At the eighth grid point, the control norm falls below the minimum threshold, indicating an invalid point for LCvx.

The accuracy of the convex solver is crucial in demonstrating the effectiveness of the perturbation strategy and the bisection search method.

6.1 Well-Conditioned Example

We begin our first example by considering an optimization problem with a four-dimensional state and a two-dimensional control. We choose $N = 10$ temporal grids, resulting in eleven state vectors $\{x_1, x_2, x_3, \dots, x_{11}\}$ and ten control vectors $\{u_1, u_2, \dots, u_{10}\}$. We use the notation $x_{i,j}$ to denote the j -th dimension of the vector x_i . In the continuous dynamics, we have $t_f = 10$ and

$$A_c = \begin{pmatrix} 0_{2 \times 2} & I_{2 \times 2} \\ 0_{2 \times 2} & 0_{2 \times 2} \end{pmatrix}, \quad B_c = (0_{2 \times 2}, I_{2 \times 2})^\top,$$

thus the discretized dynamics are given by

$$A = I_{4 \times 4} + A_c \quad B = (0.5I_{2 \times 2}, I_{2 \times 2})^\top.$$

The object function is $x_{11,3}^2 + x_{11,4}^2 + \sum_{i=1}^{11} \sigma_i$. The functions g_1 and g_2 are the squared L_2 norms; $\rho_{\min} = 1$ and $\rho_{\max} = 2$; $x_{\text{init}} = [1, 2, 3, 4]^\top$ and the boundary condition is $(x_{11,1}, x_{11,2}) = [1, 1]^\top$. In summary, we consider:

$$\begin{aligned} \min_{x, u, \sigma} \quad & x_{11,3}^2 + x_{11,4}^2 + \sum_{i=1}^{10} \sigma_i \\ \text{s. t.} \quad & x_{i+1} = Ax_i + Bu_i, \quad i \in [1, 10]_{\mathbb{N}} \\ & 1 \leq \sigma_i, \quad \|u_i\|^2 \leq \sigma_i, \quad \|u_i\| \leq 2, \quad i \in [1, 10]_{\mathbb{N}} \\ & x_1 = [1, 2, 3, 4]^\top, \quad (x_{11,1}, x_{11,2}) = [1, 1]^\top \end{aligned} \quad (5)$$

The solution trajectory and the magnitude of the controls are available in Figure 1. We observe that LCvx is invalid at the eighth temporal grid. Hence, the solution to Problem 4 does not always satisfy the constraints in Problem 3, even for a well-conditioned problem.

6.2 Artificial normal example

In this section, we consider a three-dimensional problem with $N = 10$, $A = \text{diag}(1.2, -2.2, 1)$, and $B = (0.4, 0.3, 0.2)^\top$. Notice that A and B forms a controllable

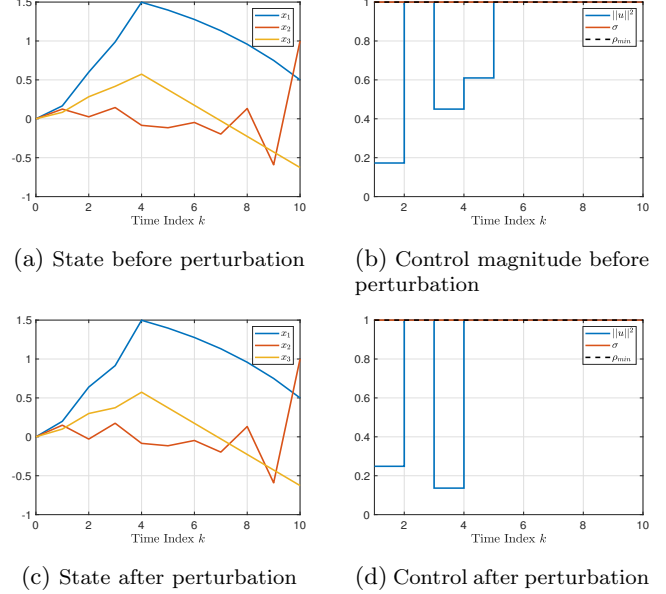


Fig. 2. System dynamics and control response before and after perturbation for an artificial three-dimensional problem with $N = 10$ temporal grid points. The top figures display the state trajectory and control magnitude prior to perturbation, revealing LCvx invalid at three points. The bottom figures show the system's response to a perturbation designed as per Theorem 20, which reduces the number of nonconvex constraint violations to two. The state variable remains essentially unchanged.

matrix pair.

$$\begin{aligned} \min_{x, u, \sigma} \quad & x_{10,3} + \sum_{i=1}^{11} \sigma_i \\ \text{s. t.} \quad & x_{i+1} = Ax_i + Bu_{i-1}, \quad i \in [1, 10]_{\mathbb{N}} \\ & x_{\text{init}} = [0, 0, 0]^\top, \quad x_{11,1} = 0.5, \quad x_{11,2} = 1 \\ & 1 \leq \sigma_i, \quad \|u_i\|^2 \leq \sigma_i, \quad \|u_i\| \leq 2, \quad i \in [1, 10]_{\mathbb{N}} \end{aligned}$$

Here, the dynamics do not come from any continuous system, as A has negative eigenvalues. This counterexample is formed by making the matrix Λ in the proof of Theorem 20 singular. The numerical tolerance for Mosek is set to 10^{-15} . The solution trajectory is available in Figure 2a, and the magnitude of the control is shown in Figure 2b. We observe that LCvx is invalid at three points. According to Theorem 20, adding a perturbation to the dynamics reduces the violation of nonconvex constraints to at most two points. We consider the following dynamics with $A_p = \text{diag}(10^{-7}, 0, 0)$:

$$x_{i+1} = (A + A_p)x_i + Bu_{i-1}, \quad i \in [1, 10]_{\mathbb{N}}$$

which introduces a small change to one element in the dynamics matrix. We maintain the numerical tolerance at 10^{-15} . The updated trajectory and control sequence are available in Figure 2c and Figure 2d, respectively. As expected, LCvx is invalid at two points after perturbation.

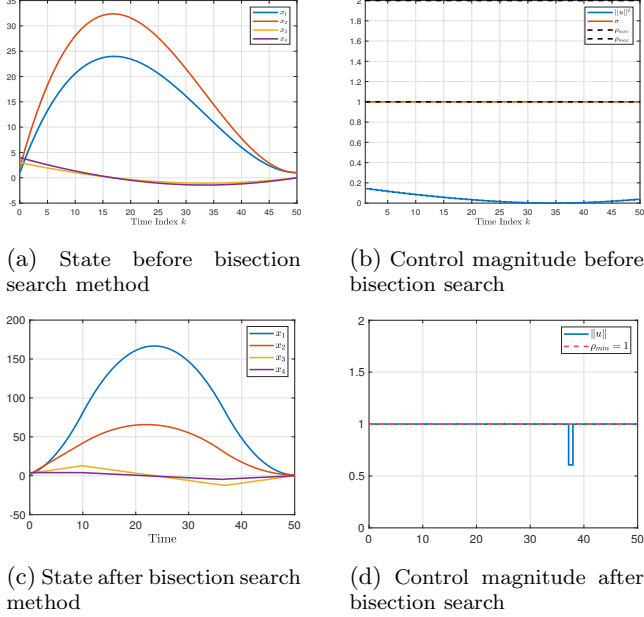


Fig. 3. State trajectory and control magnitude before and after applying the bisection search method in a long-horizon optimization scenario with $N = 50$ and $t_f = 50$. The initial figures indicate a long-horizon state where the control magnitudes are below the threshold $\rho_{\min} = 1$. The latter figures demonstrate the effectiveness of the bisection search method algorithm 1, resulting in a trajectory that LCvx violation at one point. The information for σ is not available after the perturbation.

6.3 Long-horizon example

Our final example is a long-horizon case. It follows the same setup as in example (5), with the distinction that we have $N = 50$ and $t_f = 50$. The trajectory and control magnitude are available in Figures 3a and 3b. These figures show that $x_{N,3} = x_{N,4} = 0$ and all control magnitudes are less than $\rho_{\min} = 1$, confirming that this is indeed a long-horizon case.

Now, we apply the bisection search method algorithm 1, setting $\epsilon_t = 10^{-5}$ and the initial control as $[1, 0]^\top$. The algorithm terminates with $t_{\text{high}} = 9.86$. This suggests maintaining the initial control for 9.86 units of time before starting a control sequence generated by (5). The resulting trajectory and control magnitude are shown in Figures 3c and 3d. The final state is $x_{N+1} = (1, 1, 10^{-8}, 3 \times 10^{-9})$, with all σ_i equal to 1 up to the computational error tolerance. The control magnitude plot reveals one LCvx invalidation.

7 Conclusion

In this paper, we develop a new Lossless Convexification (LCvx) method and provide theoretical guarantees for its application to discrete-time nonconvex optimal control problems, addressing a gap in the existing LCvx literature. Specifically, we demonstrate that under mild assumptions, the optimal solution of the relaxed convex problem satisfies the constraints of the original nonconvex problem at all but at most $n_x - 1$ temporal grid

points when an arbitrarily small perturbation is introduced into the dynamic constraints, where n_x is the state dimension. We also introduce a bisection search method to ensure that our new LCvx method is applicable in long-horizon cases, where the existing LCvx method results in an infeasible control sequence. Additionally, the numerical examples illustrate the necessity of the perturbation and the tightness of the $n_x - 1$ upper bound, while also demonstrating the effectiveness of the bisection search method.

For future work, we aim to investigate the theoretical guarantees of applying the LCvx method to various forms of discrete-time nonconvex optimal control problems. Furthermore, we plan to extend our results to develop a lossless convexification method that ensures continuous-time constraint satisfaction [Elango et al., 2024].

8 Appendix

8.1 Proof of theorem 8

PROOF. Let y^* be the optimal solution to Problem 6 at p_0 , satisfying assumptions in Lemma 7. The existence of y^* is a consequence of the compactness of Ω and the continuity of the object function. Lemma 7 ensures the existence of $\delta > 0$ and $\xi > 0$ such that for any $p \in \mathbb{R}^{n_p}$ with $\|p - p_0\| < \xi$, there is a point $y \in \Omega$, $F(y, p) = 0$ and

$$\|y - y^*\| \leq \frac{\|F(y^*, p)\|}{\delta}.$$

Hence, the feasible set for Problem 6 is nonempty for p sufficiently close to p_0 . Additionally, because Ω is a compact set, optimal solutions exist for Problem 6 for p sufficiently close to p_0 .

We first prove that $\liminf_{s \rightarrow p_0} M^*(s) \geq M^*(p_0)$. Consider a sequence $s_k \in \mathbb{R}^{n_p}$ sufficiently close to p_0 such that $\lim_k M^*(s_k) = \liminf_{s \rightarrow p_0} M^*(s)$ and $\lim_k s_k = p_0$. We denote the optimal solution of the Problem 6 generated by s_k as y_k . Due to the compactness of Ω , there exist a convergent subsequence y_{k_n} and a variable \bar{y} such that $\lim_n y_{k_n} = \bar{y}$ and $\liminf_{s \rightarrow p_0} M^*(s) = \lim_n M^*(s_{k_n}) = \lim_n M(y_{k_n}, s_{k_n})$. Due to the continuity of $F(y, p)$ and the closedness of Ω , \bar{y} is feasible for Problem 6 generated by p_0 . Thus, $\lim_n M^*(s_{k_n}) = \lim_n M(y_{k_n}, s_{k_n}) = M(\bar{y}, p_0) \geq M^*(p_0)$ by the continuity of $M(\cdot, \cdot)$.

Next, we aim to show that $\limsup_{w \rightarrow p_0} M^*(w) \leq M^*(p_0)$. As the object function $M(y, p)$ is locally Lipschitz and y lies in a compact set, there exists a Lipschitz constant L_M for all feasible (y, p) when $\|p - p_0\| < \xi$.

Consider a sequence w_k such that $\lim_k M^*(w_k) = \limsup_{w \rightarrow p_0} M^*(w)$ with $\|w_k - p_0\| < \xi$ and $\lim_k w_k = p_0$. Lemma 7 ensures the existence of a corresponding sequence $y_k \in \Omega$ that $F(y_k, w_k) = 0$,

$$\|y_k - y^*\| \leq \frac{\|F(y^*, w_k)\|}{\delta},$$

and $M^*(w_k) \leq M(y_k, w_k)$. Therefore,

$$\begin{aligned} \limsup_{w \rightarrow p_0} M^*(w) &= \lim_k M^*(w_k) \\ &\leq \limsup_k M(y_k, w_k) \\ &\leq \limsup_k (M(y^*, w_k) + L_M \|y_k - y^*\|) \end{aligned} \quad (6)$$

$$\begin{aligned} &\leq M(y^*, p_0) + L_M \limsup_k \frac{\|F(y^*, w_k)\|}{\delta} \\ &= M(y^*, p_0) + \frac{\|F(y^*, p_0)\|}{\delta} = M^*(p_0). \end{aligned} \quad (7)$$

Here, inequality (6) is due to the Lipschitz property of M and inequality (7) is due to the continuity of F .

In summary, we have

$$\limsup_{p \rightarrow p_0} M^*(p) \leq M^*(p_0) \leq \liminf_{p \rightarrow p_0} M^*(p),$$

thus establishing the continuity of M^* . \square

8.2 Proof for Lemma 17

Since Assumption 2 trivially holds, we start by showing the validity of Assumptions 3 and 5.

Lemma 28 *Suppose that Assumptions 3 and 5 hold for Problem 8 at $q = 0$. Then, there exists an $\epsilon > 0$ such that for any $q \in \mathbb{R}^d$ within the cube $\epsilon\mathbb{D} \in \mathbb{R}^d$, where $\mathbb{D} \subset \mathbb{R}^d$ is a unit cube, both assumptions are satisfied for Problem 8 generated by q .*

PROOF. The proof of both assumptions relies on the fact that the determinant of a matrix is a continuous function of elements in that matrix. We demonstrate Assumption 3 for Problem 8, while the nonsingularity of $\nabla_z \tilde{H}$ in Assumption 5 follows similarly and thus is omitted.

Define

$$S(q) := \begin{pmatrix} B & \tilde{A}(q)B & \dots & \tilde{A}(q)^{n_x-1}B \end{pmatrix}.$$

We aim to show that $S(q)$ retains full rank for all q within $\epsilon\mathbb{D}$. $S(q)$ has full rank if and only if the determinant of $S(q)S(q)^\top$ is nonzero. As the elements in matrix \tilde{A} are continuous functions of q , the elements and, consequently, the determinant of $S(q)S(q)^\top$ are continuous functions of q . Given that $\tilde{A}(0) = A$, the controllability of the matrix pair $\{A, B\}$ ensures that $S(0)$ has full rank and that the determinant of $S(0)S(0)^\top$ is nonzero. Through continuity, an $\epsilon > 0$ exists such that for any q within $\epsilon\mathbb{D}$, the determinant of $S(q)S(q)^\top$ remains nonzero, and $S(q)$ maintains full rank. The existence of ϵ is a corollary of [Rudin, 1964, Theorem 4.8]. \square

Now, we turn to prove that Assumption 6 holds after perturbation. To simplify the notation for Problem 8, we let $z = (x, u, \sigma)$. The object function $\Phi(z)$ and the set \tilde{V} formed by inequalities are the same as in (2). The affine constraint function $H(z)$ in (2) is augmented to $\tilde{H}(z, q)$ to accommodate the dynamics and boundary

constraints of Problem 8. Thus, our perturbed problem can be represented as:

$$\begin{aligned} \min_z \quad &\Phi(z) \\ \text{s.t.} \quad &\tilde{H}(z, q) = 0, \quad z \in \tilde{V}, \end{aligned}$$

When $q = 0$, we have $\tilde{H}(z, 0) = H(z)$, thereby retrieving the original Problem 5.

Since we need lemma 7 and theorem 8 for our discussion, we must demonstrate that their assumptions are valid.

Lemma 29 *Assumption 5 and Assumption 6 for Problem 4 ensures that for any vector z_0 such that*

$$\tilde{H}(z_0, 0) = 0, \quad z_0 \in \tilde{V},$$

we have that $y = 0$ is the unique solution of the following equation:

$$0 \in \nabla_z \tilde{H}(z_0, 0)^\top y + N_{\tilde{V}}(z_0)$$

PROOF. We prove this statement by contradiction. Assume there exists $y \neq 0$ such that

$$0 \in \nabla_z \tilde{H}(z_0, 0)^\top y + N_{\tilde{V}}(z_0).$$

Consider the function $g(z) = y^\top \tilde{H}(z, 0) + I_{\tilde{V}}(z)$, where $I_{\tilde{V}}(z)$ is the indicator function for the set \tilde{V} . Thus we have $0 \in \partial g(z_0)$ and $\tilde{H}(z_0, 0) = 0$. Since $g(z)$ is a convex function, the minimum of $g(z)$ is zero, achieved at z_0 .

Given Assumption 6, there exists an interior point z' in \tilde{V} where $\tilde{H}(z', 0) = 0$ and $N_{\tilde{V}}(z') = \{0\}$. Therefore, z' is also a minimizer of the function g , and thus $0 \in \partial g(z') = y^\top \nabla_z \tilde{H}(z', 0)$. Meanwhile, $\nabla_z \tilde{H}(z', 0) = \nabla_z \tilde{H}(z_0, 0)$ because \tilde{H} is an affine function of variable z . Consequently, the vector y lies in the left null space of $\nabla_z \tilde{H}(z, 0)$, which contradicts Assumption 5. \square

Now, we are ready to prove that Assumption 6 holds after perturbation:

Lemma 30 *Suppose that Assumption 5 and 6 hold for Problem 8 when $q = 0$. Then, there exists an $\epsilon > 0$ such that for any $q \in \mathbb{R}^d$ within the cube $\epsilon\mathbb{D} \in \mathbb{R}^d$, where $\mathbb{D} \in \mathbb{R}^d$ is a unit cube, such that the perturbed Problem 8 with respect to q also satisfies Assumption 6.*

PROOF. Slater's assumption implies the existence of a z_0 such that $H(z_0) = \tilde{H}(z_0, 0) = 0$, while z_0 lies in the interior of \tilde{V} . Since Lemma 29 ensures the applicability of Lemma 7, there exist $\epsilon_1 > 0$ and $\delta > 0$ such that for all $\|q\| < \epsilon_1$, there exists a $z(q)$, determined by q , satisfying

$$\|z(q) - z_0\| \leq \frac{\|\tilde{H}(z_0, q)\|}{\delta},$$

and $\tilde{H}(z(q), q) = 0$, thus meeting the dynamics and boundary conditions of Problem 8. Given that \tilde{H} is a continuous function, there exists an $\epsilon > 0$, such that when $\|q\| < \epsilon$, $\|z(q) - z_0\|$ is sufficiently small for $z(q)$ to lie in the interior of \tilde{V} , thereby validating Slater's condition for the perturbed problem. \square

Now we show that the perturbed problem is normal.

Lemma 31 *Suppose that Assumptions 2, 5, 6 and 14 hold for Problem 8 and $q = 0$. Then there exists an $\epsilon > 0$ such that for any q within the cube $\epsilon\mathbb{D}$, Assumption 14 is still valid for Problem 8 after perturbation by q .*

PROOF. We apply Theorem 8 to show that the optimum value of Problem 8 is continuous with respect to q . To satisfy the theorem's assumptions, we introduce a sufficiently large trivial upper bound on σ , ensuring the compactness of \tilde{V} . Assumption 2 guarantees that the optimal solution remains unchanged with or without this upper bound. Consequently, Assumption 2 and Lemma 29 confirm the validity of assumptions to Theorem 8.

Since when $q = 0$ Problem 4 is normal, the optimal value of Problem 4 is larger than $m^* + \sum_{i=1}^N l_i(\rho_{\min})$, where m^* is the minimum value of Problem 7. Thus, the continuity of the optimal value function ensures the existence of an $\epsilon > 0$ such that for all $q \in \epsilon\mathbb{D}$, the optimal value of Problem 8 generated by $\{\tilde{A}(q), B\}$ is greater than $m^* + \sum_{i=1}^N l_i(\rho_{\min})$. Assumption 2 ensures that l_i are monotone, indicating that the perturbed problem is still normal. \square

8.3 Proof for Theorem 20

The following is a useful linear algebra theorem from [Chen, 1984, Theorem 3.5] that aids us in proving Theorem 20.

Theorem 32 *Consider a function $f(\lambda)$ and a matrix $A \in \mathbb{R}^{n \times n}$. The characteristic polynomial of A is*

$$\Delta(\lambda) = \det(I - \lambda A) = \prod_{i=1}^d (\lambda - \lambda_i)^{m_i},$$

where m_i are the algebraic multiplicity of eigenvalue λ_i , $n = \sum_{i=1}^d m_i$, and d is the total number of distinct eigenvalues.

There exists a polynomial $h(\lambda)$ as

$$h(\lambda) := v_0 + v_1\lambda + \dots + v_{n-1}\lambda^{n-1}, \quad (8)$$

such that

$$f(A) = h(A).$$

The unknown coefficients of (8) are found by solving n equations:

$$f^{(l)}(\lambda_i) = h^{(l)}(\lambda_i) \text{ for } l \in [0, m_i - 1]_{\mathbb{N}}, i \in [1, d]_{\mathbb{N}}, \quad (9)$$

where

$$f^{(l)}(\lambda_i) := \left. \frac{d^l f(\lambda)}{d\lambda^l} \right|_{\lambda=\lambda_i},$$

and $h^{(l)}(\lambda_i)$ is defined in the same manner.

Now we start the proof for 20.

PROOF. [Proof for Theorem 20] If $n_x > N$, the statement holds trivially; thus, we assume $n_x \leq N$. We choose $\epsilon > 0$ sufficiently small that Lemma 17 is valid. Thus, the perturbed Problem 8 has controllable dynamics, is normal, and satisfies Slater's condition.

Consider the matrix

$$S(q) := \left(\tilde{A}(q)^{P_1} B \tilde{A}(q)^{P_2} B \dots \tilde{A}(q)^{P_{n_x}} B \right),$$

for specific integers $1 \leq P_1 < P_2 < \dots < P_{n_x} < N + 1$, where N is the total number of grid points in Problem 8, $\tilde{A}(q)$ is the perturbation of A with respect to q and n_x is the state dimension.

According to Lemma 19, if $S(q)$ is of full rank, then the Problem 8 generated by $\{\tilde{A}(q), B\}$ satisfies LCvx at least at one point among the set $\{N - P_1, N - P_2, \dots, N - P_{n_x}\}$.

We aim to demonstrate that $S(q)$ is of full rank with probability one, regardless of the choice of P_1 to P_{n_x} .

According to Theorem 32, all powers of the matrix $\tilde{A}(q)$ can be written as polynomials of $\tilde{A}(q)$ up to the power $n_x - 1$, where n_x is the dimension of the state vector x and of A . Then, there exists a matrix $V(q) \in \mathbb{R}^{n_x \times n_x}$ such that

$$\tilde{A}^{P_i}(q) = \sum_{j=1}^{n_x} V_{ij}(q) \tilde{A}^{j-1}(q), \quad i \in [1, n_x]_{\mathbb{N}}$$

Here, V_{ij} represents the element in the i -th row and j -th column of $V(q)$.

Now we show that $V(q)$ being invertible is sufficient for $S(q)$ to be of full rank: Let $W(q)$ be the inverse of $V(q)$, Then

$$\tilde{A}^i(q) = \sum_{j=1}^{n_x} W_{ij} \tilde{A}^{j-1}(q), \quad i \in [1, n_x]_{\mathbb{N}} \quad (10)$$

If $S(q)$ has a nonzero left null vector ξ , we have $\xi \tilde{A}(q)^{P_i} B = 0$ for all $i \in [1, n_x]_{\mathbb{N}}$. Equation (10) implies that $\xi \tilde{A}^i(q) B = 0$, for all $i \in [0, n_x - 1]_{\mathbb{N}}$ contradicting controllability ensured by Lemma 17.

Therefore, $V(q)$ being invertible is sufficient for $S(q)$ to be of full rank. We thus have

$\text{Prob}(\text{rank}(S(q)) < n_x) \leq \text{Prob}(V(q) \text{ being singular})$
The rest of this proof is to show that the probability on the right-hand side is zero.

Setting the distinct eigenvalues of A as $\lambda_1, \lambda_2, \dots, \lambda_d$, the eigenvalues of the perturbed matrix $\tilde{A}(q)$ have eigenvalues $\tilde{\lambda}_i = \lambda_i + q_i$ for $i \in \{1, 2, \dots, d\}$. Here, d is the number of distinct eigenvalues of A .

We start by exploring how $V(q)$ is determined by the eigenvalues $\tilde{\lambda}_i = \lambda_i + q_i$. The characteristic polynomial of A can be written as: $\prod_{i=1}^d (\lambda - \lambda_i)^{m_i}$ where $\sum_{i=1}^d m_i = n_x$ with m_i being the algebraic multiplicity of λ_i .

Due to the perturbation preserving the Jordan form, the characteristic polynomial of \tilde{A} becomes:

$$\prod_{i=1}^d (\lambda - \tilde{\lambda}_i)^{m_i} = \prod_{i=1}^d (\lambda - \lambda_i - q_i)^{m_i},$$

where $\sum_{i=1}^d m_i = n_x$. It is clear that the probability of

$$\tilde{\lambda}_i = \lambda_i + q_i = \lambda_j + q_j = \tilde{\lambda}_j$$

holding for any i and j is zero. Consequently, we retain d distinct eigenvalues with probability one.

According to Theorem 32, $V(q)$ consists of the coefficients in (8) for each P_i . For the P_i power of $\tilde{A}(q)$ and an eigenvalue $\tilde{\lambda}_j$, the equation (9) for the i -th row of $V(q)$ is:

$$\begin{aligned} \tilde{\lambda}_j^{P_i} &= V_{i1} + V_{i2}\tilde{\lambda}_j + \cdots + V_{in_x}\tilde{\lambda}_j^{n_x-1}, \\ P_i\tilde{\lambda}_j^{P_i-1} &= 0 + V_{i2} + \cdots + V_{in_x}(n_x-1)\tilde{\lambda}_j^{n_x-2}, \\ &\vdots \\ \prod_{k=0}^{m_j-2} (P_i-k)\tilde{\lambda}_j^{P_i-m_j+1} &= 0 + \cdots + V_{in_x} \prod_{k=1}^{m_j-1} (n_x-k). \end{aligned}$$

Combining all equations for different P_i and $\tilde{\lambda}_j$, there are in total n_x^2 unknown variables in $V(q)$ and n_x^2 equations. We now write all equations into a matrix equality.

For the P_i -th power and the j -th eigenvalue, to simplify the notation, we define Λ_{ij} as

$$T_j = \begin{bmatrix} \tilde{\lambda}_j^{P_i}, P_i\tilde{\lambda}_j^{P_i-1}, \dots, \prod_{k=0}^{m_j-2} (P_i-k)\tilde{\lambda}_j^{P_i-m_j+1} \end{bmatrix},$$

$$\begin{bmatrix} 1 & 0 & \cdots & 0 \\ \tilde{\lambda}_j & 1 & \cdots & 0 \\ \tilde{\lambda}_j^2 & 2\tilde{\lambda}_j & \cdots & 0 \\ \vdots & \vdots & \ddots & \vdots \\ \tilde{\lambda}_j^{n_x-1} & (n_x-1)\tilde{\lambda}_j^{n_x-2} & \cdots & \prod_{k=1}^{m_j-1} (n_x-k)\tilde{\lambda}_j^{n_x-m_j} \end{bmatrix},$$

and

$$V_i = [V_{i1}, V_{i2}, \dots, V_{in_x}].$$

Thus, we have $\Lambda_{ij} = V_i T_j$. Stacking Λ and T into matrices, we have

$$\Lambda = \begin{bmatrix} \Lambda_{11} & \Lambda_{12} & \cdots & \Lambda_{1d} \\ \vdots & \vdots & \ddots & \vdots \\ \Lambda_{n_x 1} & \Lambda_{n_x 2} & \cdots & \Lambda_{n_x d} \end{bmatrix}$$

and

$$T = [T_1, T_2, \dots, T_d].$$

According to Theorem 32, the matrix $V(q)$ must satisfy

$$\Lambda = VT,$$

where Λ , V , and T are n_x -by- n_x matrices and functions of q . The determinant of Λ is the product of the determinants of V and T . Hence, for V to be singular, Λ must also be singular.

We establish the non-singularity of Λ through induction. To begin, we construct a sequence of matrices $C_k \in \mathbb{R}^{M_k \times M_k}$, for $k = 1, 2, \dots, d$ and $M_k = \sum_{i=1}^k m_i$. Each C_k is designed to be a square matrix formed from the top-left corner of the matrix Λ . Specifically C_k is de-

finied as:

$$C_k = \begin{bmatrix} \Lambda_{11} & \cdots & \Lambda_{1k} \\ \vdots & & \\ \Lambda_{M_k 1} & \cdots & \Lambda_{M_k k} \end{bmatrix}_{M_k \times M_k}.$$

As $n_x = \sum_{i=1}^d m_i$, where d is the number of distinct eigenvalues that A has, it follows that $C_d = \Lambda$.

We initiate induction by proving that the probability of C_1 being singular is zero. Substituting the expression of Λ_{ij} into the definition of C_1 , we obtain:

$$C_1 = [\Lambda_{11}^\top, \Lambda_{21}^\top, \dots, \Lambda_{M_1 1}^\top]^\top = \begin{bmatrix} \tilde{\lambda}_1^{P_1} & P_1\tilde{\lambda}_1^{P_1-1} \cdots & \prod_{r=0}^{m_1-2} (P_1-r)\tilde{\lambda}_1^{P_1-m_1+1} \\ \vdots & & \\ \tilde{\lambda}_1^{P_{m_1}} & P_{m_1}\tilde{\lambda}_1^{P_{m_1}-1} \cdots & \prod_{r=0}^{m_1-2} (P_{m_1}-r)\tilde{\lambda}_1^{P_{m_1}-m_1+1} \end{bmatrix}.$$

The determinant of C_1 is computed as a sum of signed products of matrix entries. Each summand in this sum represents a product of distinct entries, with no two entries sharing the same row or column. Consequently, all summands contribute to the same power order of $\tilde{\lambda}_1$. Therefore, the determinant of C_1 can be expressed as:

$$\det(C_1) = c_1 \tilde{\lambda}_1^{\sum_{r=1}^{m_1} P_r - \sum_{r=1}^{m_1} (r-1)},$$

with constant c_1 .

The expression for c_1 can be found by setting $\tilde{\lambda}_1 = 1$, as this expression for C_1 holds for all realizations of $\tilde{\lambda}_1$. We denote E_1 as the matrix that generates c_1 , that is, $c_1 = \det(E_1)$. Each element in E_1 is a polynomial in P_i , where $i \in \{1, 2, \dots, m_1\}$. Notably, the polynomials in the same column share the same coefficients. This structure allows E_1 to be transformed into a Vandermonde matrix through column transformations. Given that P_i are distinct, this Vandermonde matrix is nonsingular, implying $c_1 \neq 0$. Thus C_1 is nonsingular as long as $\tilde{\lambda}_1 \neq 0$. Given that $\tilde{\lambda}_1$ follows a uniform distribution, the probability of $\tilde{\lambda}_1 = 0$ is zero. Therefore, C_1 is nonsingular with probability one.

Now, assuming that C_k is nonsingular with probability one, we show that C_{k+1} is also nonsingular with probability one. We start by showing that with fixed values of $\tilde{\lambda}_1, \tilde{\lambda}_2, \dots, \tilde{\lambda}_k$ and the condition that C_k being nonsingular, the conditional probability of C_{k+1} being nonsingular is one. Partition C_{k+1} into the following blocks:

$$\begin{bmatrix} C_k & D_{k+1} \\ R_{k+1} & S_{k+1} \end{bmatrix}.$$

Here, $R_{k+1} \in \mathbb{R}^{m_{k+1} \times M_k}$ does not contain $\tilde{\lambda}_{k+1}$, and $D_{k+1} \in \mathbb{R}^{m_{k+1} \times M_k}$ contains terms involving $\tilde{\lambda}_{k+1}$ up to

order P_{M_k} . The terms of $\tilde{\lambda}_{k+1}$ with power higher than P_{M_k} are all included in $S_{k+1} \in \mathbb{R}^{m_{k+1} \times m_{k+1}}$.

Given the fixed values of $\tilde{\lambda}_1, \tilde{\lambda}_2, \dots, \tilde{\lambda}_k$, the determinant $\det(C_{k+1})$ becomes a polynomial in $\tilde{\lambda}_{k+1}$ with fixed coefficients. The term with the highest power in this polynomial arises from the product of elements in C_k with elements in S_{k+1} . The absolute value of the highest power term is in fact $|\det(C_k) \det(S_{k+1})|$.

Note that the matrix S_{k+1} shares the same pattern as C_1 . Following a similar line of reasoning as in the case of E_1 , we can conclude that the coefficient of $\det(S_{k+1})$ is also nonzero. Since C_k is nonsingular, the determinant $\det(C_{k+1})$ has a nonzero leading term, implying that it has a finite number of roots. Meanwhile, the distribution of $\tilde{\lambda}_{k+1}$ is a uniform distribution independent of previous eigenvalues. Therefore, the conditional probability of $\tilde{\lambda}_{k+1}$ coinciding with these roots i.e.

$\text{Prob}(C_{k+1} \text{ singular} | C_k \text{ nonsingular}, (\tilde{\lambda}_1, \dots, \tilde{\lambda}_k) \text{ fixed})$

is zero. Note that $\text{Prob}(\tilde{\lambda}_1, \tilde{\lambda}_2, \dots, \tilde{\lambda}_k | C_k \text{ nonsingular})$ is a uniform distribution over the domain of $\tilde{\lambda}_1, \tilde{\lambda}_2, \dots, \tilde{\lambda}_k$, which is the set $\epsilon \mathbb{D}$ projected to the first k dimensional minus a measure zero set representing perturbations that make C_k singular. By integrating into $\tilde{\lambda}_1, \tilde{\lambda}_2, \dots, \tilde{\lambda}_k$, we deduce that:

$$\text{Prob}(C_{k+1} \text{ singular} | C_k \text{ nonsingular}) = 0.$$

Thus $\text{Prob}(C_{k+1} \text{ singular}) = 0$, as c_k is nonsingular with probability one.

Using induction, $\Lambda = C_d$ is nonsingular with probability one, which implies that V is also nonsingular. Consequently, $S(q)$ has full rank with probability one. Due to the discussion at the start of this proof, the probability of LCvx being invalid at all grid points $(N - P_1, N - P_2, \dots, N - P_{n_x})$ is zero. This means that, for any selection of n_x grid points, the probability of simultaneously violating the original nonconvex constraints at these points is zero. Hence, the probability of at least n_x violations of the original nonconvex constraints is also zero. \square

8.4 Proof for Theorem 22

PROOF. Since $\tilde{A}^i(\cdot)$ is a smooth function of the perturbation and the matrix norm is a Lipschitz function, there exists an ϵ_1 such that $\|\tilde{A}^i(\cdot)\|$ is a Lipschitz function for perturbations $\|q\| \leq \epsilon_1$ and for $i = 0, 1, 2, \dots, N-1$. Let L_A denote the maximum Lipschitz constant among all i of $\|\tilde{A}^i(\cdot)\|$. Additionally, Assumption 2 ensures that $u_i(q)$ is bounded, i.e., $\max \|u_i(q)\| < D$ for some $D > 0$. Therefore, when $\|q\| \leq \epsilon_1$, we can compare $\tilde{x}_{N+1}(q)$ with

$x_{N+1}(q)$, and obtain:

$$\begin{aligned} & \|\tilde{x}_{N+1}(q) - x_{N+1}(q)\| \\ &= \left\| \sum_{i=1}^N (\tilde{A}^{i-1}(0) - \tilde{A}^{i-1}(q)) B u_i(q) \right\| \\ &\leq \sum_{i=1}^N L_A \|q\| \|B\| \|u_i(q)\| \leq N D L_A \|B\| \|q\|. \end{aligned}$$

Hence, $\tilde{x}_{N+1}(q)$ locates in a local neighborhood of $x_{N+1}(q)$ with radius $N D L_A \|B\| \epsilon_1$. Meanwhile, since G is an affine function and $G(x_{N+1}(0)) = 0$, we have $\|G(\tilde{x}_{N+1}(q))\| < \delta$, for sufficiently small $\|q\|$.

Now we move on to the second result. Since the control is bounded, $x(q)$ is bounded. Thus, $m(\cdot)$ in Problem 8 is a Lipschitz function within the domain of x because m is C^1 smooth. with Lipschitz constant L_m . Thus:

$$|m(\tilde{x}_{N+1}(q)) - m(x_{N+1}(q))| \leq N D L_A L_m \|B\| \|q\|.$$

Meanwhile, Lemma 29, Lemma 31 (for the compactness), and Theorem 8 indicate that the optimum value of Problem 8 is continuous with respect to q . Therefore, for any $\delta > 0$ there exists $\epsilon > 0$ such that for all $\|q\| < \epsilon$,

$$\begin{aligned} & m(\tilde{x}_{N+1}(q)) + \sum_{i=1}^N l_i(g_1(u_i(q))) \\ &\leq m(x_{N+1}(q)) + \sum_{i=1}^N l_i(g_1(u_i(q))) + K_q \|q\| \\ &\leq m(x_{N+1}(0)) + \sum_{i=1}^N l_i(g_1(u_i(0))) + K_q \|q\| + \delta/2 \\ &\leq m_o^* + K_q \|q\| + \delta/2, \end{aligned}$$

where $K_q = N D L_A L_m \|B\|$. Here, the second inequality arises from Theorem 8 that the optimum value of Problem 8 is continuous with respect to q , and that $(u(0), x_{N+1}(0))$ is the solution to the unperturbed problem. The last inequality is derived from the fact that the optimum value of Problem 4 lower bounds that of Problem 3. Hence, for sufficiently small $\|q\|$, we have $m(\tilde{x}_{N+1}(q)) + \sum_{i=1}^N l_i(g_1(u_i(q))) \leq m_o^* + \delta$. \square

8.5 Proof for Theorem 27

PROOF.

Denote $(x(q), u(q), \sigma(q))$ the solution to Problem 10 generated by t_s^* and perturbed by q . For any $\epsilon > 0$, we set $\eta = \min\{\epsilon L_l(t_f - t_s^*)/N, \frac{3\epsilon}{4}\}$. According to Theorem 26, there exists a t_s^* such that

$$\begin{aligned} v(t_s^*) &= m(x_{N+1}(0)) + \frac{t_f - t_s^*}{N} \sum_{i=1}^N l(\sigma_i(0)) \\ &\quad + t_s^* l(\rho_{\min}) \leq m^* + t_f l(\rho_{\min}) + \frac{\eta}{2} \end{aligned}$$

where m^* is the optimum of Problem 7 and $x_{N+1}(0)$ is the result of the unperturbed Problem 10 formed by t_s^* .

The first result follows from Theorem 22. The second result is from Theorem 20 as long as we choose δ sufficiently small such that $\|q\| \leq \delta$ is included in the cube area defined by Theorem 20. We now proceed to prove the third and fourth results.

According to Lemma 31,

$$m(x_{N+1}(q)) + \frac{t_f - t_s^*}{N} \sum_{i=1}^N l(\sigma_i(q)) + t_s^* l(\rho_{\min})$$

is a continuous function of q in a neighborhood of zero. Therefore, there exists a $\delta > 0$ such that for all $\|q\| \leq \delta$,

$$\begin{aligned} m(x_{N+1}(q)) + \frac{t_f - t_s^*}{N} \sum_{i=1}^N l(\sigma_i(q)) \\ \leq v(t_s^*) - t_s^* l(\rho_{\min}) + \frac{\eta}{2} \\ \leq m^* + (t_f - t_s^*) l(\rho_{\min}) + \eta. \end{aligned}$$

Since $x_{N+1}(q)$ is feasible for the perturbed problem, we have $G(x_{N+1}(q)) = 0$ and $x_{N+1}(q)$ is feasible for Problem 7. Therefore, $m(x_{N+1}(q)) \geq m^*$ and

$$\frac{\sum_{i=1}^N l(\sigma_i(q))}{N} \leq \frac{\eta}{t_f - t_s^*} + l(\rho_{\min}).$$

As $\sigma_i(q) \geq \rho_{\min}$ for all i and l has positive derivative, we have

$$l(\rho_{\min}) \leq l(\sigma_i(q)) \leq l(\rho_{\min}) + \frac{N\eta}{t_f - t_s^*}.$$

Given that $\eta \leq \epsilon L_l (t_f - t_s^*)/N$ and the derivative of l is larger than L_l , we have

$$|\sigma(q) - \rho_{\min}| \leq \frac{N\eta}{L_l(t_f - t_s^*)} \leq \epsilon,$$

yielding the third result.

For the final result, since $l(\rho_{\min}) \leq l(\sigma_i(q))$, we have

$m(x_{N+1}(q)) \leq m^* + \eta$. Furthermore, Theorem 22 indicates that

$$|m(\tilde{x}_{N+1}(q)) - m(x_{N+1}(q))| \leq NDL_AL_M\|B\|\|q\|,$$

where D , L_A , and L_M are defined in Theorem 22 and are constants when t_s^* is fixed. Thus, we obtain

$$m(\tilde{x}_{N+1}(q)) \leq m^* + \eta + NDL_AL_M\|B\|\|q\|.$$

With a sufficiently small $\|q\|$, we have $m(\tilde{x}_{N+1}(q)) \leq m^* + \epsilon$. \square

References

Behçet Açıkmeşe and Scott Ploen. A powered descent guidance algorithm for mars pinpoint landing. In *AIAA Guidance, Navigation, and Control Conference and Exhibit*, page 6288, 2005.

Behçet Açıkmeşe and Scott Ploen. Convex programming approach to powered descent guidance for mars landing. *Journal of Guidance, Control, and Dynamics*, 30(5):1353–1366, 2007.

Behçet Açıkmeşe, Jordi Casoliva, John M Carson, and Lars Blackmore. G-fold: A real-time implementable

fuel optimal large divert guidance algorithm for planetary pinpoint landing. *Concepts and Approaches for Mars Exploration*, 1679:4193, 2012.

Behçet Açıkmeşe, M Aung, Jordi Casoliva, Swati Mohan, Andrew Johnson, Daniel Scharf, David Masten, Joel Scotkin, Aron Wolf, and Martin W Regehr. Flight testing of trajectories computed by G-FOLD: Fuel optimal large divert guidance algorithm for planetary landing. In *AAS/AIAA spaceflight mechanics meeting*, page 386, 2013.

Behçet Açıkmeşe and Lars Blackmore. Lossless convexification of a class of optimal control problems with non-convex control constraints. *Automatica*, 47(2): 341–347, 2011.

MOSEK ApS. *The MOSEK optimization toolbox for MATLAB manual. Version 9.0.*, 2019. URL <http://docs.mosek.com/9.0/toolbox/index.html>.

HH Bauschke. Convex analysis and monotone operator theory in hilbert spaces, 2011.

Leonard D. Berkovitz. *Optimal Control Theory*. Springer-Verlag, 1975. doi: <https://doi.org/10.1007/978-1-4757-6097-2>.

Jonathan Borwein and Adrian Lewis. *Convex Analysis*. Springer, 2006.

Stephen P Boyd and Lieven Vandenberghe. *Convex optimization*. Cambridge university press, 2004.

Michael D Canon, Clifton D Cullum Jr, and Elijah Polak. *Theory of optimal control and mathematical programming*. McGraw-Hill, 1970.

John M Carson, Behçet Açıkmeşe, and Lars Blackmore. Lossless convexification of powered-descent guidance with non-convex thrust bound and pointing constraints. In *Proceedings of the 2011 American Control Conference*, pages 2651–2656. IEEE, 2011.

Chi-Tsong Chen. *Linear system theory and design*. Saunders college publishing, 1984.

Francis Clarke. *Functional analysis, calculus of variations and optimal control*, volume 264. Springer, 2013.

Francis H Clarke, Yuri S Ledyaev, Ronald J Stern, and Peter R Wolenski. *Nonsmooth analysis and control theory*, volume 178. Springer Science & Business Media, 2008.

A. Domahidi, E. Chu, and S. Boyd. ECOS: An SOCP solver for embedded systems. In *2013 European Control Conference (ECC)*, pages 3071–3076, 2013.

Kazuya Echigo, Christopher R. Hayner, Avi Mittal, Selahattin Burak Sarsilmaz, Matthew W. Harris, and Behçet Açıkmeşe. Linear programming approach to relative-orbit control with element-wise quantized control. *IEEE Control Systems Letters*, 7:3042–3047, 2023. doi: 10.1109/LCSYS.2023.3289472.

Kazuya Echigo, Abhishek Cauligi, and Behçet Açıkmeşe. Expected time-optimal control: a particle model predictive control-based approach via sequential convex programming, 2024. Available at <https://arxiv.org/abs/2404.16269>.

Purnanand Elango, Dayou Luo, Samet Uzun, Taewan Kim, and Behçet Açıkmeşe. Successive convexification for trajectory optimization with continuous-time con-

- straint satisfaction. *arXiv preprint arXiv:2404.16826*, 2024.
- Matthew Fritz, Javier Doll, Kari C Ward, Gavin Mendeck, Ronald R Sostaric, Sam Pedrotty, Chris Kuhl, Behçet Açıkmeşe, Stefan R Bieniawski, Lloyd Strohl, et al. Post-flight performance analysis of navigation and advanced guidance algorithms on a terrestrial suborbital rocket flight. In *AIAA SCITECH 2022 Forum*, page 0765, 2022.
- Matthew W. Harris. Optimal control on disconnected sets using extreme point relaxations and normality approximations. *IEEE Transactions on Automatic Control*, 66(12):6063–6070, 2021. doi: 10.1109/TAC.2021.3059682.
- Matthew W Harris and Behçet Açıkmeşe. Lossless convexification for a class of optimal control problems with linear state constraints. In *52nd IEEE Conference on Decision and Control*, pages 7113–7118. IEEE, 2013.
- Matthew W Harris and Behçet Açıkmeşe. Lossless convexification of non-convex optimal control problems for state constrained linear systems. *Automatica*, 50(9):2304–2311, 2014.
- Sheril Kunhippurayil, Matthew W Harris, and Olli Jansson. Lossless convexification of optimal control problems with annular control constraints. *Automatica*, 133:109848, 2021.
- Donggun Lee, Shankar A Deka, and Claire J Tomlin. Convexifying state-constrained optimal control problem. *IEEE Transactions on Automatic Control*, 68(9):5608–5615, 2022.
- Danylo Malyuta, Taylor P Reynolds, Michael Szmuk, Thomas Lew, Riccardo Bonalli, Marco Pavone, and Behçet Açıkmeşe. Convex optimization for trajectory generation: A tutorial on generating dynamically feasible trajectories reliably and efficiently. *IEEE Control Systems Magazine*, 42(5):40–113, 2022.
- Arkadi Nemirovski. Interior point polynomial time methods in convex programming. *Lecture notes*, 42(16):3215–3224, 2004.
- Sina Ober-Blobbaum, Oliver Junge, and Jerrold E Marsden. Discrete mechanics and optimal control: an analysis. *ESAIM: Control, Optimisation and Calculus of Variations*, 17(2):322–352, 2011.
- Walter Rudin. *Principles of mathematical analysis*, volume 3. McGraw-hill New York, 1964.
- Suresh P. Sethi. *Optimal Control Theory: Applications to Management Science and Economics*. Springer Texts in Business and Economics. Springer, 4 edition, 2021. ISBN 978-3-030-91744-9.
- Joshua Shaffer, Chris Owens, Theresa Klein, Andrew D Horchler, Samuel C Buckner, Breanna J Johnson, John M Carson, and Behçet Açıkmeşe. Implementation and testing of convex optimization-based guidance for hazard detection and avoidance on a lunar lander. In *AIAA SciTech 2024 forum*, page 1584, 2024.